Behaviour of Geosynthetic Reinforced Soil (GRS) Wall as a Bridge Abutment Using Numerical Analysis

Pelluru Venkata Pavan Kumar

Civil Engineering
National Institute of Technology Rourkela

Behaviour of Geosynthetic Reinforced Soil (GRS) Wall as a Bridge Abutment Using Numerical Analysis

Thesis submitted in partial fulfillment

of the requirements of the degree of

Master of Technology

in

Geotechnical Engineering

by

Pelluru Venkata Pavan Kumar

(Roll Number: 215CE1016)

based on research carried out

under the supervision of

Dr. Ramakrishna Bag

and

Dr. Shantanu Patra

May, 2017

Department of Civil Engineering

National Institute of Technology Rourkela

Department of Civil Engineering
National Institute of Technology Rourkela

May 28, 2017

Certificate of Examination

Roll Number: *215CE1016*

Name: *PELLURU VENKATA PAVAN KUMAR*

Title of Thesis: ***Behaviour of Geosynthetic Reinforced Soil (GRS) Wall as a Bridge Abutment Using Numerical Analysis***

We the below signed, after checking the thesis mentioned above and the official record book(s) of the student, hereby state our approval of the thesis submitted in partial fulfillment of the requirements of the degree of Master of Technology in Geotechnical Engineering at National Institute of Technology Rourkela. We are satisfied with the volume, quality, correctness, and originality of the work.

_____

Dr. Ramakrishna Bag
Supervisor

_____

Head of the department

Department of Civil Engineering
National Institute of Technology Rourkela

Dr. Ramakrishna Bag
Assistant Professor

May 28, 2017

Supervisor's Certificate

This is to certify that the work presented in the thesis entitled "***Behaviour of Geosynthetic Reinforced Soil (GRS) Wall as a Bridge Abutment Using Numerical Analysis****",* Roll Number 215CE1016, is a record of original research carried out by him under my supervision and guidance in partial fulfillment of the requirements for the degree of *Master of Technology in Geotechnical Engineering.* Neither this thesis nor any part of it has been submitted earlier for any degree or diploma to any institute or university in India or abroad.

Dr. Ramakrishna Bag
Assistant Professor

Dedicated to my lovable parents and my sister

Declaration of Originality

I, Pelluru Venkata Pavan Kumar, Roll Number 215CE1016 hereby declare that this thesis entitled "***Behaviour of Geosynthetic Reinforced Soil (GRS) Wall as a Bridge Abutment Using Numerical Analysis****"* presents my original work carried out as a postgraduate student of NIT Rourkela and, to the best of my knowledge, contains no material previously published or written by another person, nor any material presented by me for the award of any degree or diploma of NIT Rourkela or any other institution. Any contribution made to this research by others, with whom I have worked at NIT Rourkela or elsewhere, is explicitly acknowledged in the thesis. Works of other authors cited in this thesis have been duly acknowledged under the section "Reference". I have also submitted my original research records to the scrutiny committee for evaluation of my thesis.

I am fully aware that in the case of any non-compliance detected in future, the senate of NIT Rourkela may withdraw the degree awarded to me on the basis of the present thesis.

May 28, 2017

NIT Rourkela *Pelluru Venkata Pavan Kumar*

Acknowledgement

I would like to express my heartfelt gratitude to my supervisors **Dr. Ramakrishna Bag,** Department of Civil Engineering NIT Rourkela and **Dr. Shantanu Patra**, Department of Civil Engineering IIT Mandi for their guidance, supervision, encouragement and constant support throughout my thesis work.

I would like to extend my gratefulness to **Dr. S. K. Sahu,** Head of the Civil Engineering Department, National Institute of Technology, Rourkela, for providing the necessary facilities for my thesis work.

I want to express my respect to my committee members and for their generous help in various ways for the completion of this thesis.

I am thankful to all the faculty members of the Department of Civil Engineering, National Institute of Technology, Rourkela for helping me during the thesis period.

I would like to thank all my friends for their encouragement and help in all ways possible to think beyond the observable. Without their companionship the completion of my thesis would have been tough.

I am greatly indebted to my parents for their continuous support that helped me at every step of life. Their sincere blessings and wishes have enabled me to complete my work successfully.

May, 2017 *Pelluru Venkata Pavan kumar*

NIT Rourkela Roll Number: 215CE1016

Abstract

Reinforced soil walls (RSW) are the cost effective soil retaining walls and are gaining popularity now a days. The factors influencing the use of these walls includes economical, simple and fast construction techniques, better seismic performance. The use of GRS walls as bridge abutment is an alternative to the conventional use of deep foundation systems to support the bridge abutment. These effectively reduce the differential settlement arising between the bridge abutment and the approach roadway and this is called as the 'bump at the bridge problem'. To check the stability of these structures the Limit equilibrium methods are commonly used because of its simplicity. Mostly these methods are empirical in nature and they don't consider actual soil reinforcement interaction. Finite element method (FEM) and limit analysis (LA) methods are effective in finding the stability of a structure. The present study, discusses the numerical analysis of a full scale reinforced soil wall using commercially available software's PLAXIS 2D and LimitState:GEO. The deformation and safety analysis has been carried out for the RSW by considering a surcharge on it which can be simulated as a bridge abutment. The effect of different parameters such as unit weight and the angle of internal friction of the; length of the reinforcement; the number of reinforcement; and interface coefficient between backfill and reinforcement on the performance of the GRS wall has been studied. The surcharge is applied on the wall with a certain setback distance (D) in terms of the height of the wall (H). From the analysis it is found that the friction angle of the backfill has the maximum contribution in increasing the factor of safety (FOS) of the wall. Two different case studies have been taken for the analysis and the results obtained from numerical study are in comparison with that of the measured values.

Keywords: Reinforced soil wall, finite element method, limit analysis, bridge abutment, deformation, safety analysis.

Contents

List of Figures

List of Tables

Chapter 1

Introduction

1.1 Origin of the project

The soil reinforcement is one of the ways to stabilize the soil by the use of geotextiles, geogrids, metallic strips etc. In this, the reinforcement is embedded in the soil which takes almost zero tension so that the wall is stable for larger heights. The advantage is that shear resistance developed between the soil and reinforcement enhances the shear strength of soil. Now a day's most of the design is done with free draining granular soils, as in the case of cohesive soils there will be the effect of pore water which reduces the shear strength of soil. These walls are designed for the internal as well as external stability. The internal stability includes determination of tension and pullout resistance in reinforcing elements. The external stability includes determining overturning, sliding and bearing capacity failure.

The RSW's are also used in transportation systems to support the backfill soil, roadway structures, and the traffic loads. There are several factors which influence the increase in the use of soil reinforcement, includes economical, aesthetic, simple and fast construction techniques, better seismic performance and it has the ability to tolerate the differential settlements. The new application of this technology is the use of geosynthetic reinforced soil (GRS) wall as bridge abutments. In this case the reinforcement tensions and soil stresses are mobilized to higher levels compared to GRS walls supporting self-weight. When compared to the methods involving the use of deep foundations to support bridge abutments, the use of GRS systems alleviates the 'bump at the bridge' problem caused by the differential settlement between the bridge abutment and approach roadway. Some of the real time examples of reinforced soil wall are shown in figure 1.1. and figure 1.2.

Some of the real time applications of soil reinforcement include:

a) Soil retaining structures

b) Bridge abutments and wing walls

c) Roadway and railway embankments

d) Slope failure repairs

e) Slope cutting repairs

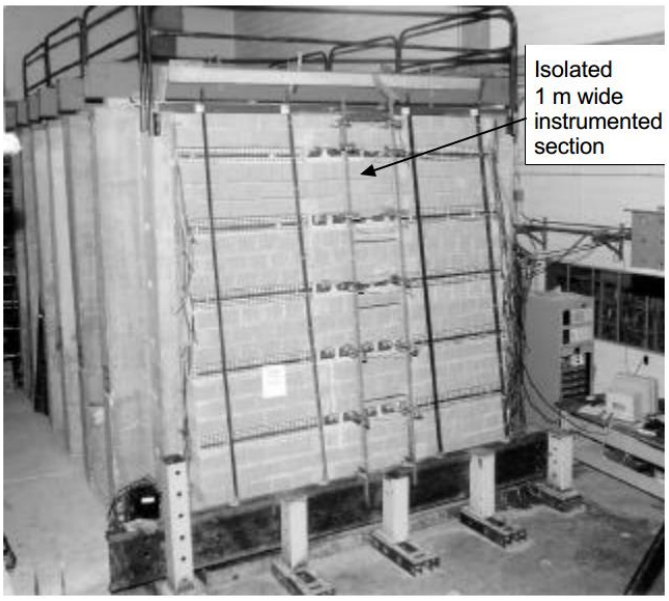

Figure.1.1: Instrumented Reinforced soil wall (Bathurst et al. 2009)

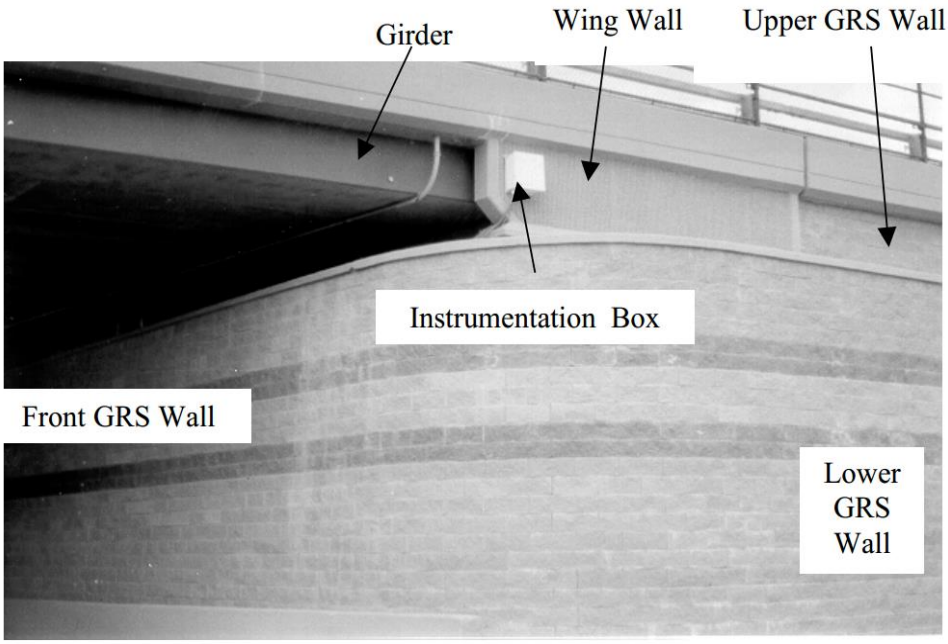

Figure.1.2: GRS wall as bridge abutment (Abu-Hejleh et al. 2002)

In the present study, the stability and deformation analysis has been carried out using finite element method (FEM) and limit analysis (LA) method. The performance of the wall with the application of a surcharge on the footing resting on the back of the wall facing at a certain setback distance is studied. The finite element method is carried out using PLAXIS 2D and the limit analysis is carried out using LimitState:GEO software packages. The LA method models the soil as a perfectly plastic material and is based on the upper-bound theorem. According to the upper bound theorem, if a set of external loads are acting on a body and the work done by external loads in an increment of displacement equals to the work done by internal stresses, and the external loads are not lower than the true collapse loads. In this the external loads are not necessarily to be in equilibrium with the internal stresses and the failure mechanism is not necessarily the actual failure mechanism.

The effect of different parameters includes; angle of internal friction of the backfill soil, length of the reinforcement, unit weight of the backfill, number of reinforcement provided, and the interface coefficient between reinforcement and the backfill was studied. The results obtained are compared between FEM and LA approach for the RSW's resting on a firm foundation. To simulate the bridge loads coming on to soil, a footing is considered on the soil wall at a setback distance (D) in terms of the height of the wall (H) from the wall facing and a surcharge is applied to it. The failure and deformation analysis were carried for different cases involving different setback distances and different backfill soil properties. Two case studies have been taken and the finite element and limit analysis are carried out which shows a good agreement between the measured values obtained from the literature.

1.2 Objective and Scope

The main objective of the project is to study the deformation behaviour and failure pattern of GRS wall as a bridge abutment for various properties of soil and setback distances.

The scope of the present study includes:

i. Parametric study of the assumed reinforced soil wall by considering various parameters such as unit weight, frictional angle, L/H ratio, the number of reinforcement etc.
ii. Calibration of the software by validating the results of a case study with that of the results obtained from PLAXIS 2D and LimitState:GEO.
iii. The behavior GRS wall is studied when it is used as a bridge abutment for different set back distances and properties of the soil.

Chapter 2

Literature Review

Various literature has been collected for the present study and the brief description is presented in the following section. There are several factors which influence the performance of the GRS wall and the effects of different properties are compiled here in literature. The present literature also includes the performance of GRS wall as a bridge abutment.

2.1 Performance of GRS wall

2.1.1 Effect of reinforcement stiffness and compaction of backfill

Hatami et al. (2001) studied a total of 21 wall models which are having different reinforcement stiffness values. The results suggested that to minimize the facing deformation, it is preferred to use the reinforcement layers with less stiffness at small spacing than the stiffer reinforcement layers at a greater spacing. The reinforcement stiffness is effective in minimizing the surface deformation when it is placed at a shallow depth (Bhandari and Han 2010).

Ehrlich et al. (2012) observed that at the end of construction the wall which is heavily compacted is having higher mobilized tension in the reinforcement compared to the wall where light compaction was used. The connection load was lesser in the wall which is compacted heavily than that of in the wall with light compaction.

2.1.2 Effect of backfill

Guler et al. (2007) studied the failure mechanisms of reinforced soil walls with extensible reinforcements by numerical analysis using finite element method. A total of 16 models with different reinforcement spacing, reinforcement length and backfill soil type were analysed. When the design loads are surpassed, the direct sliding mode is the governing failure mechanism for walls with both the granular and cohesive backfill soils when the

structure is constructed on a firm foundation. The tensile loads observed in the case of cohesive backfill were smaller than the tensile loads observed in the case of granular backfill. At the end of construction unlike in granular backfill, there was no definite shear strain concentration zone in case of cohesive backfill walls under working load conditions.

Guler and Cicek (2012) reported the effect of cohesive and granular backfill in the reinforced soil wall. The results of this study are when cohesive backfill was used the horizontal wall deformations were reduced up to 50% and the tensile forces decreased significantly.

Yu et al. (2015) studied MSE wall reinforced with steel strips constructed in Japan. The results are with the increase in backfill soil modulus there is a decrease in the tensile loads in the steel strips and in vertical facing load at the toe. The soil friction angle has the most significant factor which affects the required minimum length of reinforcement (Bilgin 2009).

2.1.3 Effect of prestressing to reinforcement

Lovisa et al. (2010) studied the behavior of the prestressed geotextile-reinforced sand bed with a loaded circular footing experimentally. The results are, for the surface footing the load carrying capacity at 5mm settlement is almost double for the prestressed case than that of reinforced sand without prestressed geotextile. The addition of prestressing to reinforcement also improved the settlement response.

Lackner et al. (2013) did experiments on 10 prestressed reinforced soil walls under static and cyclic loading. The static test results showed that there is 60% reduction in the soil layer displacements and for the cycling loading there is 80% reduction in soil layer displacements when compared to the unreinforced soil. When it comes to load displacement behavior the tensile stiffness of the reinforcement should be given an utmost importance.

2.1.4 Effect of foundation and base restraint

Rowe and skinner (2001) analysed GRS wall which is constructed on a soft foundation and rigid foundation. The wall constructed on a soft foundation increases the lateral deformation of the wall facing to around 150%, increases the vertical stress at the toe of the wall and importantly increases the strains in reinforcement layers.

Mirmoradi et al. (2014) carried out numerical analysis on GRS walls with segmental block facing with and without base restraint. They reported that for free base conditions with constant reinforcement stiffness, tension in reinforcement was independent of facing stiffness and it is same. For the fixed base, the tension mobilized in reinforcement and horizontal toe load is a function of facing stiffness.

2.2 Reinforced soil wall as bridge abutment

Fahel et al. (2000) investigated the behavior of geogrid reinforced bridge abutment built close to an existing highway embankment and the bridge in the BR-101 highway in the state of Santa Catarina, Brazil. The foundation of the bridge is of organic soft clay and the unidirectional geogrid layers were used as reinforcement in cohesion less backfill soil. The faster rate of construction of the embankment and the orientation of stiffer reinforcement layer direction along the embankment axis caused the collapse of side slope of one of the abutment. This failure can be avoided by constructing a berm along the side slope. The presence of reinforcement layers significantly reduced the lateral displacement of the foundation soil and also minimized the damages caused to existing structures.

Abu-Hejleh et al. (2002) monitored a two-span bridge and approaching roadway which is supported by GRS wall near Denver, Colorado, USA. They have evaluated the deformation response of the Founders/Meadows bridge abutments under service loads based on the displacement data collected through surveying, strain gauges, and digital road profiler. The observation is, the monitored displacements are smaller than those expected. There are no signs of differential settlements and the bump at the bridge. The post construction outward displacements were small with time and it is at a decreasing rate.

Helwany et al. (2003) conducted finite element analysis using the computer program DACSAR. The effect of different foundations soils includes loose sand to stiff clay on the performance of GRS bridge abutment were studied. The use of dense sand as foundation material reduced the outward displacements of the segmental wall and it is maximum at mid-height of the wall. In the case of medium dense to loose sand the maximum wall displacements were observed at the bottom of the wall. When the foundation soil is weak the lateral outward displacements are more at the bottom of the wall and therefore the strains in the bottom geosynthetic layers were increased. In the case of stiff and medium stiff clay the outward displacements are small and are occuring at the mid-height of the wall. The

differential settlement between the bridge abutment and the approach embankment were observed to be very small.

Skinner and Rowe (2005) considered a hypothetical GRS wall of 6m height which supports bridge abutment and approaching roadway constructed on the 10 m thick yielding clayey soil. They have examined the effect of yielding clayey soil deposit on the behaviour of the wall and abutment. In this case two different loading conditions were taken: the first is considering the abutment and road dead loads, the second is considering the traffic loads in addition to the dead loads. The total vertical and horizontal displacements were larger at the top of the wall than at the base. The vertical stress predicted at the base of the wall was lower than the stress calculated from the design except at the toe, which is 29% higher than the designed values in both the cases 1 and 2. The increase in the length and stiffness of bottom reinforcement layer has very little effect on increasing the bearing capacity of the wall but on stiffening these layers the local and undrained shear deformation were reduced, however, the settlements are large.

Wu et al. (2006) conducted finite element analysis using finite element program DYNA3D on the GRS bridge abutment with the flexible facing. The study was carried out on the allowable bearing pressure of bridge sills over the GRS abutments. The effect of sill type, sill width, soil stiffness, reinforcement spacing, and the foundation stiffness on the load carrying capacity of GRS abutment sills was analysed. For the determination of allowable bearing pressure two performance criteria were employed: limiting displacement criterion and limiting shear strain criterion. It is observed that the allowable bearing pressure from limiting displacement criterion are somewhat smaller than those from limiting shear strain criterion for a reinforcement spacing of 0.2m. For the reinforcement spacing of 0.4m, there occurs a facing failure with the increase in the applied pressure. The sill settlement in the case of the integrated sill is smaller than that of the isolated sill, whereas the maximum lateral displacement of the wall facing for both the sill types was almost same.

Grien et al. (2010) analysed the effect of thermal deformation of the integral bridge deck on a mechanically stabilized earth (MSE) wall using FLAC 2D, particularly the induced tensile force in reinforcement and deformation of facing wall due to movement of the bridge. The vertical stress below the footing is varying depending on the horizontal displacement of the bridge. They have observed the tensile forces in the reinforcement at all levels in case of standard bridge abutment are higher than the integral bridge abutment for both thermal

expansion and contraction. There is an inward movement of the abutment in the case of standard bridge abutments, this unexpected lateral movement is one of the cause for the increase in tensile stress and lateral movement compared to the integral bridge abutments, where there is a lateral constraint provided by bridge deck.

Zheng and Fox (2016) numerically studied the performance of GRS bridge abutments under static footing loading. The effects of different parameters like backfill soil cohesion; backfill soil relative compaction; reinforcement spacing, length and stiffness; bridge contact friction coefficient and the bridge load were studied. The backfill soil relative compaction, reinforcement spacing, and the bridge loads have the greater influence on the lateral facing displacements and the bridge footing settlements. For a given superstructure load the abutment deflections can be reduced by increasing the reinforcement length and stiffness, increasing the bridge contact friction coefficient, increasing backfill soil relative compaction. The backfill soil cohesion has a significant effect in controlling the lateral facing displacements but in the case of bridge footing settlement it is not so. For the design to be conservative in many cases zero cohesion is assumed.

Chapter 3

Theory

3.3 Finite Element Method (PLAXIS 2D)

PLAXIS 2D is a commercial finite element package used for the 2-D analysis of deformation and stability problems in geotechnical engineering and it is equipped with different types of features to deal with complex geotechnical structures. In the present study the modelling has been carried out with 2-D plane strain condition and a 15-noded triangular element has been chosen for the materials considered.

The Mohr-Coulomb model is considered for the modelling of the soil, this requires five input parameters, namely Young's modulus (E in kN/m^2), Poisson's ratio (μ), cohesion (c in kN/m^2), angle of internal friction (φ in degrees), and a dilatancy angle (ψ in degrees). When the geometry is fully defined and the material properties are assigned to all the clusters and structural objects, the mesh has been generated which divides the whole model into a number of discrete triangular elements. During the calculation process the displacements (u_x and u_y) are calculated at the nodes, and these nodes can be pre-selected for the generation of load-displacement curves. The stresses and strains are calculated at Gaussian integration points or stress points rather than at nodes (Guler et. al 2012).

The factor of safety (FOS) is computed from PLAXIS 2D using the *phi-c reduction* approach. In this approach the strength parameters φ and *c* of soil are successively reduced until failure occurs. While calculation the strength parameters are automatically reduced until the final calculation step and thus results in fully developed failure mechanism. If interfaces are used this strength also reduced in the same way. In PLAXIS the total multiplier $\sum \boldsymbol{Msf}$ is used to define the soil strength parameters at a given stage and is define as follows.

$$\sum Msf = \frac{\tan\varphi_{input}}{\tan\varphi_{reduced}} = \frac{c_{input}}{c_{reduced}}$$

Here the subscript 'input' refers to the properties given in the material sets and the subscript 'reduced' refers to the reduced values used in the analysis. The *phi-c reduction* calculation

is performed using the procedure *load advancement number of steps* defined in PLAXIS. It must be checked always whether the final step has resulted in a fully developed failure mechanism, in this case the FOS is given by:

$$SF = \frac{available\ strength}{strength\ at\ failure} = value\ of\ \sum Msf\ at\ failure$$

If the failure mechanism not fully developed then the calculation should be repeated with larger number of steps.

For the load controlled calculations PLAXIS has the provision of using *arc-length* control procedure, which is by default selected for *plastic* calculation or *phi-c reduction* calculation to obtain the collapse loads. The iteration procedure when arc-length control is not used is shown in Figure 3.1 (a) where the collapse load is being approached. For this case the algorithm will not converge to a solution, hence the calculation will keep on iterating. If the *arc-length* control is selected, the PLAXIS will automatically measure the portion of external load that must be applied for the collapse of the structure (Figure 3.1 (b))

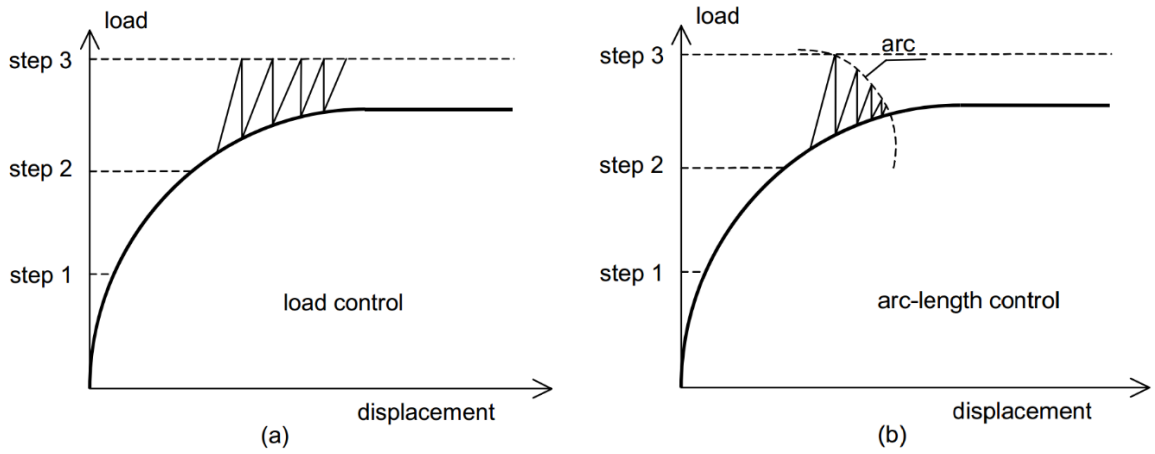

Figure.3.1. Iterative procedure for a) normal load control b) arc-length control [19]

3.4 Limit Analysis Method (LimitState:GEO)

LimitState:GEO is a 2-Dimensional software program which is designed to analyse the ultimate limit state (ULS) or collapse state for a vast variety of geotechnical problems. It directly identifies the critical collapse mechanism using the computational limit analysis technique Discontinuity Layout Optimization (DLO) and is based on upper-bound of

plasticity. The DLO uses in-depth mathematical optimization techniques to identify the critical layout of slip-lines appears at the time of failure. The DLO can be used to identify the critical translational failure mechanism for any geotechnical problem, to a user specified geometry. The solution for the problem is presented as an 'adequacy factor'. This is the factor by which the specified loads must be increased or material strengths must be reduced, in order to reach the collapse state of the system under consideration. In the case where the adequacy factor is greater than one the structure is considered to be safe. In the present study the adequacy factor on strength was selected while calculation. In the LimitState:GEO there are two types of Adequacy factor namely:

1. Adequacy factor on load
2. Adequacy factor on strength

In the case of elasto-plastic FE analysis, it requires many iterations to arrive at a ULS solution, numerical limit analysis seeks out the solution directly by merging optimization techniques and rigorous plasticity theory. LA, thus has the advantage that it can directly determine a solution and generally suffers from no numerical instabilities. LA requires only two strength parameters for any material to model, the cohesion (c) and the angle of internal friction (φ).

The reinforcement in soil is modelled using the Engineered Element material defined in LimitStat:GEO. The engineered element provided has a pullout resistance T_1 per unit length, lateral resistance against displacement of N_1 per unit length, and a plastic moment of M_{p1}. If there are m objects present per unit width, then $T = mT_1$ is the pullout resistance per unit length per unit width, and $N = mN_1$ is the resistance per unit length per unit width to lateral displacement of the objects and $M_p = mM_{p1}$. In LimitSatate:GEO the resistances T and N are computed as a linear functions of vertical effective stress at the element as follows [16]:

$$T = T_c + T_q \sigma_v'$$

$$N = N_c + N_q \sigma_v'$$

where T_c, T_q, N_c and N_q are the constants defined for the Engineered Element.

T_c is the pullout factor used to determine the contribution of material cohesion to the pullout resistance of the element.

T_q is the pullout factor used to determine the contribution of overburden to the pullout resistance of the element.

N_c is the lateral factor used to determine the contribution of material cohesion to the lateral resistance of the element.

N_q is the lateral factor used to determine the contribution of overburden to the lateral resistance of the element.

The vertical effective stress (σ_v') is computed by the LimitState:GEO prior to solving, based on the weight of overburden per unit area above the mid-point of element minus the pore pressure at the mid-point of the element.

Chapter 4

Parametric Study of Full Scale Reinforced Soil Wall

Guler et.al (2007) studied failure mechanism analysis by considering effects of type of backfill soil, reinforcement spacing, and the length of the reinforcement. They have considered a wall of height 9m placed on stiff foundation. The backfill, foundation soil and the modular blocks for the facing are considered as Mohr-Coulomb material. In general the concrete modular blocks are considered as linear-elastic material. In the present study the modular blocks are modelled as linear-elastic elements in the PLAXIS 2D.

For the calibration of the software, a GRS wall is considered and the effect of different parameters of the soil on the FOS of the wall has been found out using PLAXIS 2D and LimitState:GEO software. The cross section of the wall is shown in figure 4.1. The wall is of 6.0m in height with a cohesionless backfill resting on an unyielding foundation. A uniaxial geogrid with a high value of axial rigidity (EA=10000kN/m) is considered as the reinforcement. Appropriate interfaces are provided between soil reinforcement, facing blocks, facing block-foundation, and backfill-foundation. The facing contains 6 number of concrete blocks of thickness 0.2m and this concrete block is defined as a liner elastic element in PLAXIS 2D.

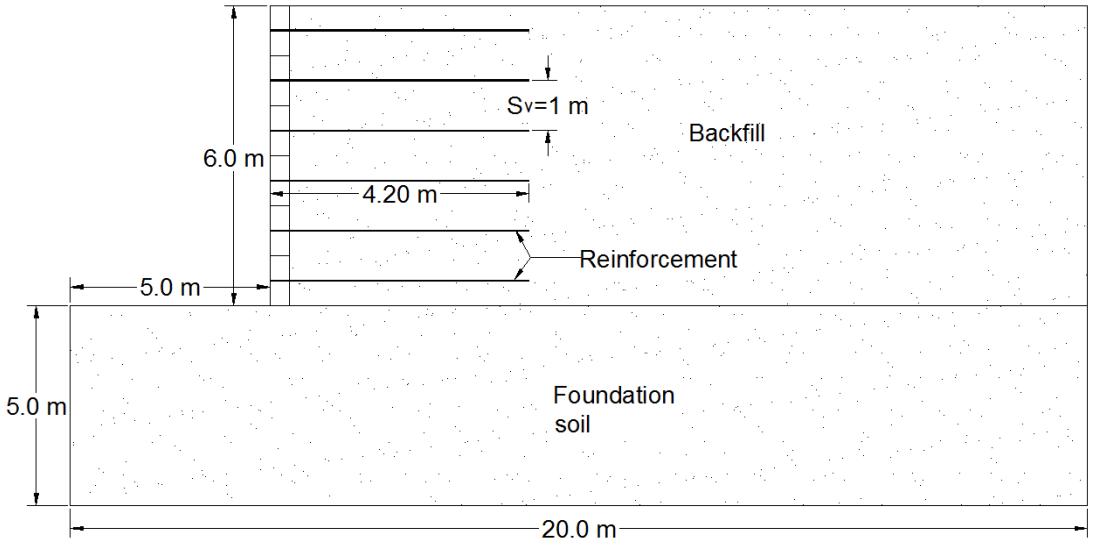

Figure 4.1: Geometry of the wall considered for parametric study

The foundation is considered as non-yielding i.e. failure in the foundation is negligible. High values of Young's modulus (E) and cohesion (c) is considered for the foundation. The standard values of the parameters for the backfill soil are unit weight (γ) is 18kN/m^3, the angle of internal friction (φ) is 30^0. The backfill soil is considered to be cohesionless soil. In order to avoid complications PLAXIS 2D recommends giving a minimum value of cohesion (c), here it is considered as 1 kN/m^2. The Young's modulus (E) is 30,000kN/m^2, Poisson's ratio (μ) is 0.3, the interface coefficient between soil and reinforcement (R_{inter}) is 0.67, L/H ratio is 0.5, and a number of reinforcement layers are 6. When calculating the FOS of one case all the others parameters are maintained constant. The range of parameters considered for the study is shown in Table 4.1. Figure 4.2. shows the finite element mesh of RSW modelled in PLAXIS 2D.

Table 4.1: Range of the parameters used for the parametric study

Property	**Value**
Model	Mohr-Coulomb
soil unit weight (kN/m^3)	16-22
Angle of internal friction, φ (degrees)	25- 55
Cohesion, c (kN/m^2)	1
Young's modulus, E_{ref} (kN/m^2)	30,000
Poisson's ratio, μ	0.3
Interface, R_{inter}	0.67-1.0
L/*H* ratio	0.4-0.8
Number of reinforcement layer, *n*	2-10

L-length of reinforcement; H-height of the wall

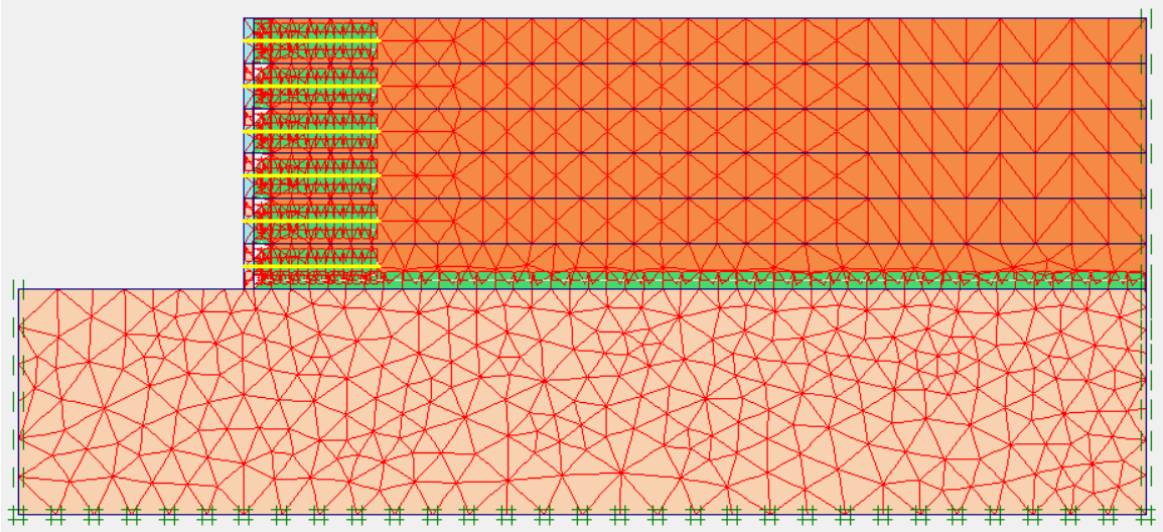

Figure 4.2: Finite element mesh of GRS wall

The bottom portion of the wall is fixed in both vertical and horizontal directions, the right side and left side boundary in fixed in horizontal direction throughout. The same backfill parameters as that of PLAXIS 2D were used in LimitState:GEO. The reinforcement parameters used in LA are shown in table 4.2.

Table.4.2: Parameters for the reinforcement used in LimitState:GEO

Property	**Value**
Pullout factor, T_c (kN/m^2)	0
Pullout factor, T_q	0.36
Lateral factor, N_c (kN/m^2)	1
Lateral factor, N_q	0
Moment of resistance, M_p (kN/m^2)	0
Rupture strength, R (kN/m)	10^{30}
Compressive strength, C (kN/m)	0

4.2 Parametric study

The factor of safety values obtained for various properties of the backfill soil from the PLAXIS 2D and LimitState:GEO are shown in table 4.3. The variation of the FOS is shown in figure 4.3.

Table.4.3: FOS's for the RSW by LA and FEM

Phi (degrees)	LA	FEM
25	1.017	-
30	1.244	1.196
35	1.495	1.427
45	2.094	1.960
55	2.876	2.673

L/H	LA	FEM
0.4	1.096	1.026
0.5	1.244	1.196
0.6	1.385	1.381
0.7	1.512	1.490
0.8	1.633	1.605

Gamma (kN/m^3)	LA	FEM
16	1.254	1.212
18	1.244	1.196
20	1.236	1.188
22	1.229	1.178

R_{inter}	LA	FEM
0.67	1.244	1.196
0.8	1.313	1.257
0.9	1.356	1.285
1	1.389	1.292

Number of reinforcement (n)	LA	FEM
2	0.9221	-
4	1.159	1.106
6	1.244	1.196
8	1.314	1.240
10	1.335	1.264

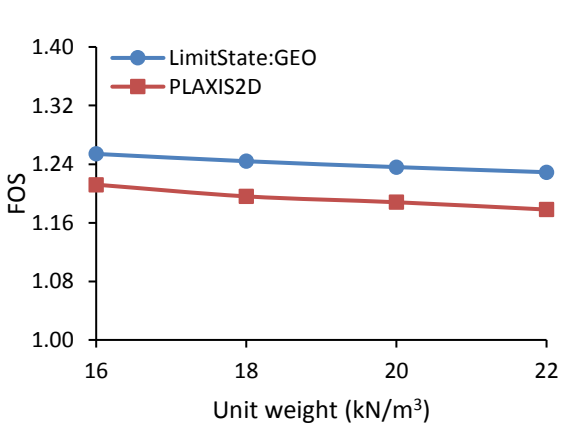

(a) Effect of unit weight

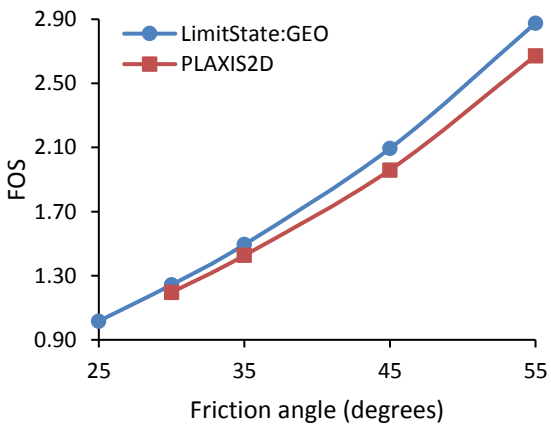

(b) Effect of friction angle

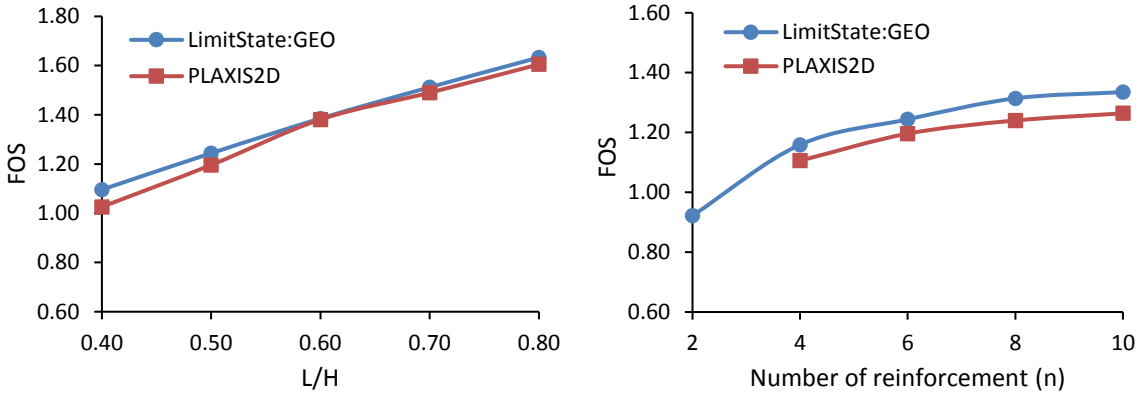

(c) Effect of L/H ratio (d) Effect of No. of Reinforcement

Figure.4.3: Effect of different parameters on FOS

The results for the parametric variation of the angle of internal friction of backfill, and L/H ratio by FEM and LA are shown in table 4.4 and table 4.5 respectively. These values are calculated for 6 number of reinforcement.

Table.4.4: FOS obtained by FEM for different L/H and friction angle

L/H	**Φ=30^0**	**Φ=35^0**	**Φ=45^0**	**Φ=55^0**
0.4	1.026	1.231	1.704	2.330
0.5	1.196	1.427	1.960	2.673
0.6	1.381	1.647	2.264	3.046
0.7	1.490	1.779	2.447	3.279
0.8	1.605	1.914	2.614	3.500

Table.4.5: FOS obtained by LA for different L/H and friction angle

L/H	**Φ=30^0**	**Φ=35^0**	**Φ=45^0**	**Φ=55^0**
0.4	1.096	1.314	1.845	2.567
0.5	1.244	1.495	2.094	2.876
0.6	1.385	1.665	2.316	3.153
0.7	1.512	1.817	2.499	3.400
0.8	1.633	1.955	2.673	3.653

The results for the parametric variation of the angle of internal friction of backfill, and number of reinforcement by FEM and LA are shown in table 4.6 and table 4.7 respectively.

Table.4.6: FOS obtained by FEM for different number of reinforcement and friction angle

Number of reinforcement (n)	**Φ=30^0**	**Φ=35^0**	**Φ=45^0**	**Φ=55^0**
4	1.106	1.318	1.81	2.49
6	1.196	1.427	1.960	2.673
8	1.240	1.476	2.03	2.766
10	1.264	1.509	2.075	2.825

Table.4.7: FOS obtained by LA for different number of reinforcement and friction angle

Number of reinforcement (n)	**Φ=30^0**	**Φ=35^0**	**Φ=45^0**	**Φ=55^0**
4	1.159	1.392	1.939	2.575
6	1.244	1.495	2.094	2.876
8	1.314	1.576	2.184	2.964
10	1.335	1.606	2.223	3.009

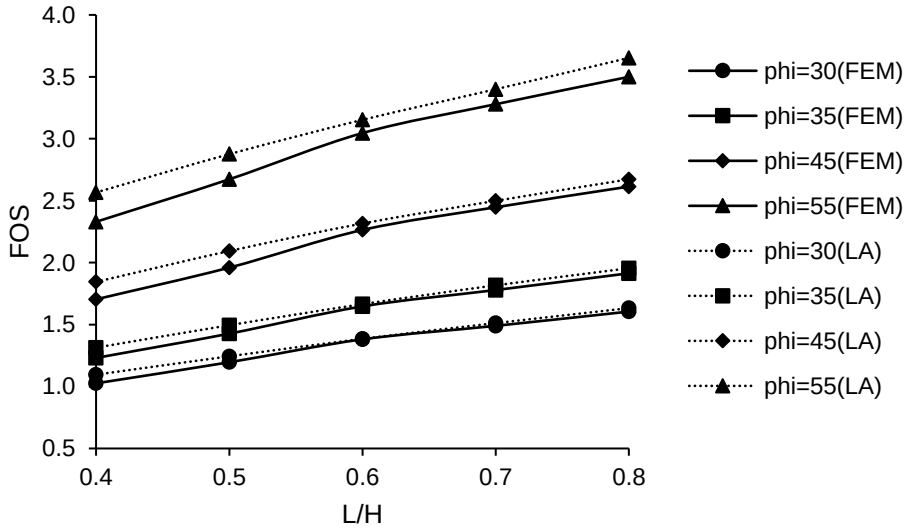

Figure.4.4: FOS for parametric variation of frictional angle of backfill and L/H ratio by FEM and LA

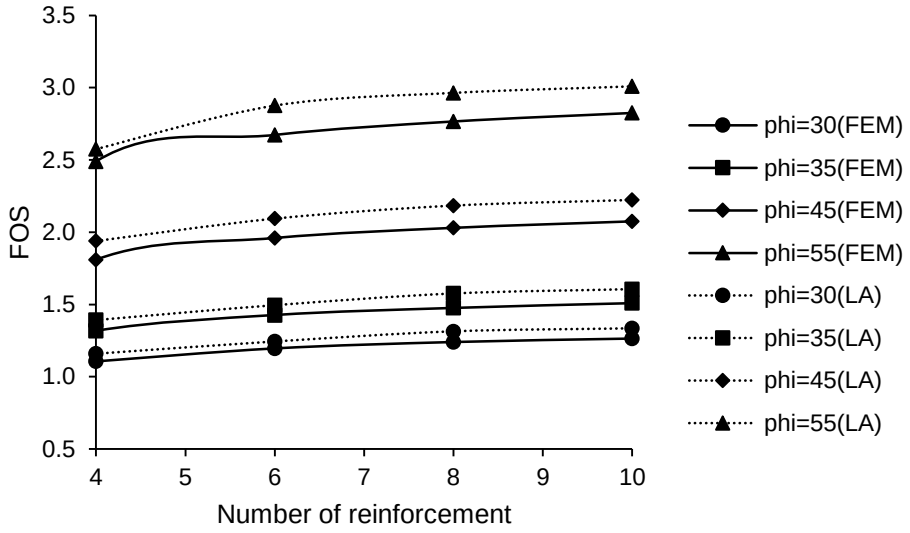

Figure.4.5: FOS for parametric variation of frictional angle of backfill and number of reinforcement by FEM and LA

It can be seen from figure 4.3 (b, c and d) that the angle of internal friction has a significant effect in increasing the FOS of the wall compared to the other parameters. For 6 number of reinforcement in the present study the FOS value decreases with the increase in the unit weight of the backfill (figure 4.3 a). This decrease in FOS is due to the inadequate length of the reinforcement provided, and the increase in unit weight of the backfill has a tendency of pushing away the wall which separates the reinforced zone from the unreinforced zone and thus causes a reduction in the FOS.

With the increase in the angle of internal friction the FOS increased linearly (figure 4.4., and figure4.5). When the angle of internal friction of the backfill is increased, the active earth pressure on the wall reduces and thus the FOS is increased. It is also observed that the increase in the length of reinforcement enhances the FOS. The increase in the length of reinforcement increases the effective length of reinforcement (L_{ei}) and thereby the increase in pull-out resistance (eq. 4.1). This increase pull-out resistance in turn increases the factor of safety.

The pull-out resistance in each layer of the reinforcement is given by the following equation (Kumar and Madhav 2009):

$$T = 2 \times \gamma \times z_i \times L_{ei} \times \tan \varphi_r \qquad (4.1)$$

where, L_{ei} is the effective length of the i^{th} layer of reinforcement located outside of failure zone, at a depth z_i from the top of the wall and φ_r is the interface friction angle.

Chapter 5

Analysis of Case Studies

5.3 Instrumented wall

A full scale modular block wall which was constructed at Royal Military College of Canada was taken for the present study (Bathurst et al. 2009). The wall is of 3.6m height with a batter angle (ω) of 8^0 which was constructed on a rigid concrete floor with polypropylene geogrid reinforcement. Figure 5.1 shows the cross-section of the wall used for the present study.

The soil is modelled as a Mohr-Coulomb material which involves five input parameters i.e. E and μ for soil elasticity, φ and c for soil plasticity and ψ as an angle of dilatancy. Table 5.1 shows the different properties of the backfill soil. A stage construction has been adopted in FEM with each lift is of 150mm thickness until the full height of the wall is reached.

Table.5.1: Properties of backfill soil (Bathurst et al. 2009)

Property	**Value**
Peak plane-strain friction angle, φ (degrees)	44
Cohesion, c (kPa)	0.1
Dilatancy, ψ (degrees)	14
Bulk unit weight, γ (kN/m^3)	16.8
Young's modulus, E (kPa)	20000
Poisons ratio, μ	0.3

This wall has been analyzed in the PLAXIS 2D to find out the reinforcement load at different heights and the facing wall displacements at the end of construction of the wall and on applying a surcharge of 50kPa. The predicted maximum reinforcement loads from FEM are then compared with the reinforcement loads calculated from AASHTO (2002)

simplified method. The calculation of maximum reinforcement loads (T_{max}) from the AASHTO method is expressed as follows:

$$T_{\max} = K(\gamma z + q)S_v$$

where, z is the depth of the reinforcement layer below the top of the wall and K is the active earth pressure coefficient, given by the following equation,

$$K = \frac{\cos^2(\varphi + \omega)}{\cos^2 \omega[1 + (\sin\varphi / \cos\omega)]^2}$$

where, φ is the angle of internal friction and ω is the batter angle

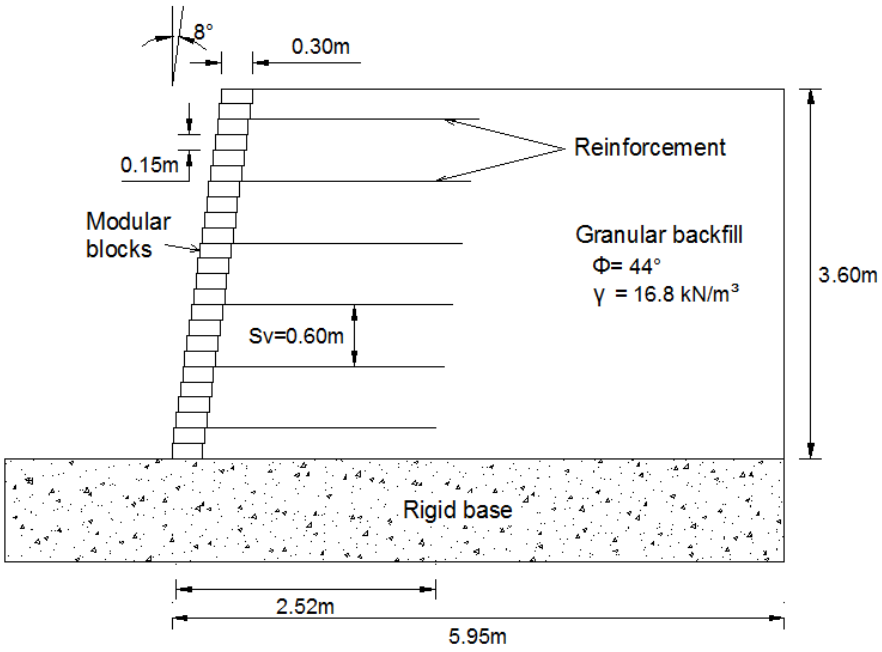

Figure.5.1: Geometry of the wall (Bathurst et al. 2009)

5.3.1 Reinforcement loads

The loads in the reinforcement obtained from the FEM are compared with the measured values, calculated values (Mirmoradi et al. 2007) and with AASHTO simplified method. The finite element values of reinforcement load are in agreement with calculated values of Mirmoradi et al. (2007) and these values are slightly higher than the measured values. Figure 5.2 shows the variation of reinforcement loads at the end of construction with the height of the wall. The maximum reinforcement load form FEM is observed to be at a height

of 0.9m from the bottom of the wall. In contrast the measured maximum reinforcement load is at bottom of the wall.

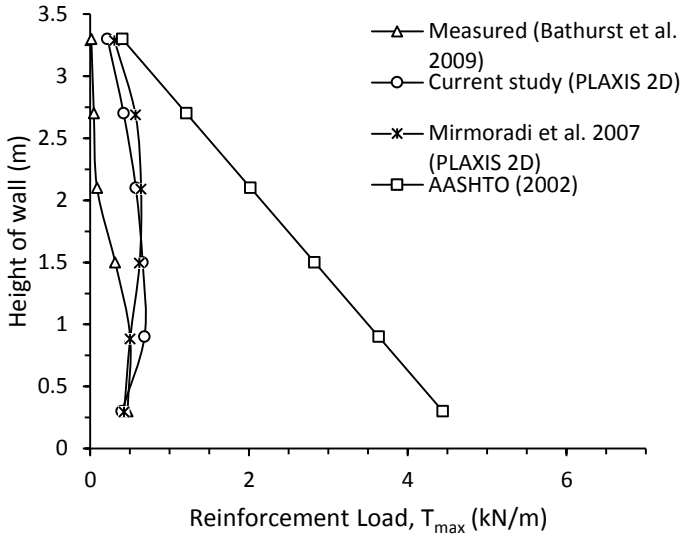

Figure.5.2: Reinforcement loads at end of construction

5.3.2 Wall facing displacements

The displacement profile of the wall is in good agreement with finite element and the measured displacement profile. At a surcharge of 50kPa the results are in good agreement with the measured values except for a deviation at the top of the wall. Figure 5.3 shows the wall facing displacement profile.

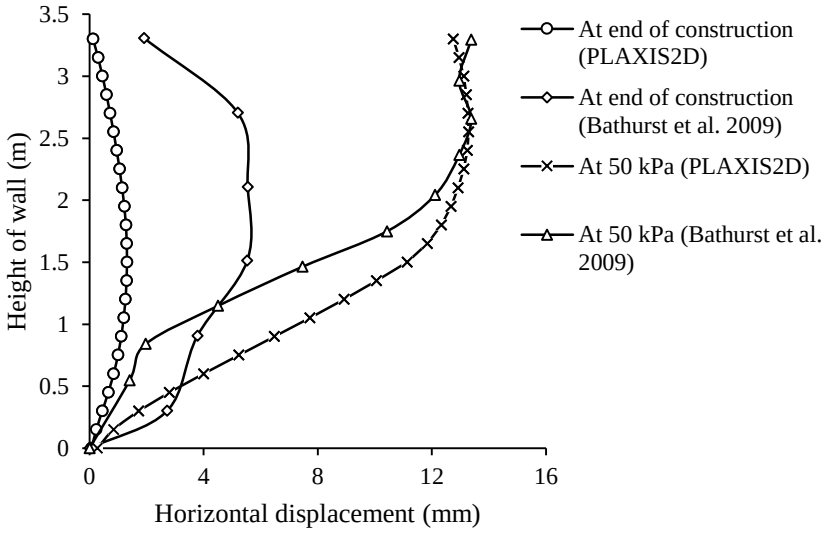

Figure.5.3: Wall facing displacement

5.4 Bridge abutment

Numerical analysis has been carried out on the founders/meadows bridge constructed near Denver in the USA. This bridge was analysed numerically during construction, after the end of construction, and in service behavior. The results obtained from the analysis were compared with the measured values (Abu-Hejleh et al. 2002). The geometry of the bridge abutment is shown in figure 5.4.

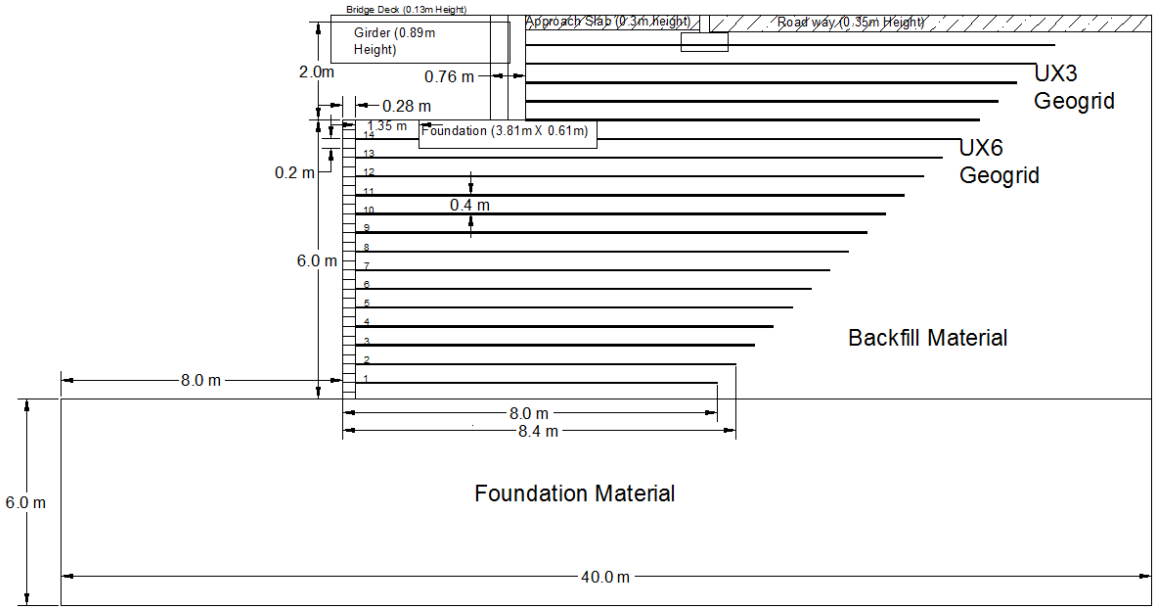

Figure.5.4: Cross-section of the Founders Bridge (Abu-Hejleh et al. 2002)

5.4.1 Material properties

The facing block, bridge footing, abutment wall, approach slab and roadway are modelled as linear elastic materials with a modulus of elasticity E=20GPa and Poisson's ratio μ=0.15. The properties of the backfill soil are shown in Table 3. The foundation soil was modelled as Mohr-Coulomb material with E=150MPa, μ=0.3, φ=35^0 and with nearly no cohesion. Three different types of geogrids are used in the construction: UX6 for the lower wall with an axial stiffens of 2000kN/m and UX3 and UX2 for the upper wall having axial stiffness 1000kN/m behind abutment.

Table.5.2: Properties of the backfill soil (Abu-Hejleh et al. 2002)

Property	Value
Model	Mohr-Coulomb
Unit weight, γ (kN/m^3)	22.1
Young's modulus, E_{ref} (kN/m^2)	50,000
Poisson's ratio (μ)	0.3
Friction angle, (degrees)	39.5
Cohesion, c (kPa)	69.8
Dilation angle, (degrees)	6

5.4.2 Modelling of the bridge

The construction procedure of the bridge was simulated using PLAXIS by modelling it in stages. The height of the each lift is taken as 0.2m which is the height of the individual facing block. The data for the bridge had been collected for the following 7 stages.

Stage 1: Construction of the lower GRS wall up to the elevation of bridge footing (5.4m)

Stage 2: Placement of the bridge footing and abutment wall, and the remaining height of the lower GRS wall (6.0m).

Stage 3: Placement of the girder.

Stage 4: Placement of backfill soil and reinforcement for the upper GRS wall behind the abutment wall.

Stage 5: Placement of the bridge deck.

Stage 6: Load due to approach slab and the roadway.

Stage 7: Loads coming on to the bridge after opening it to traffic.

5.4.3 Geogrid displacements and tensile forces

The horizontal displacements are observed in two Geogrids (Grid layer 6 and 10) which are at an elevation of 2.4m and 4.0m from the bottom at different construction stages (Figure 5.5). The measured (Abu-Hejleh et. al 2002), simulated (Zheng et. al 2016) and observed (PLAXIS 2D) maximum tensile forces in Geogrid layers 6 and 10 at the end of construction (stage 6) are shown in table 5.3.

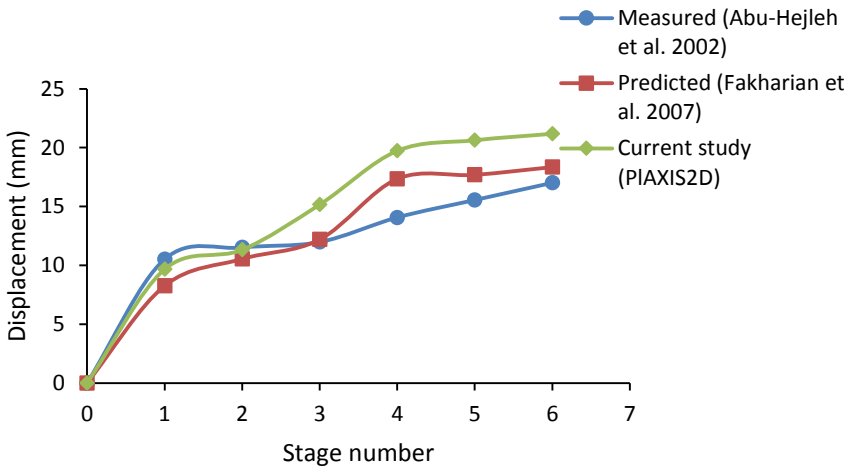

(a)

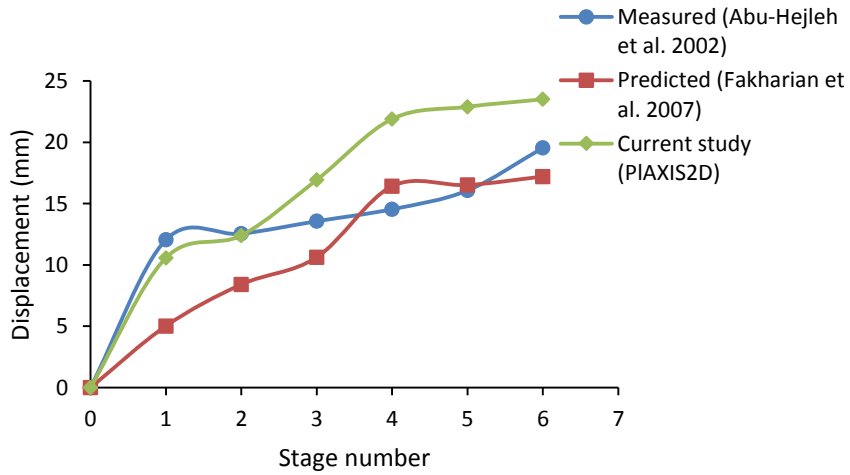

(b)

Figure.5.5: Horizontal displacements during construction

(a) Grid layer 6 and (b) Grid layer 10

Table.5.3: Tensile forces and horizontal Geogrid reinforcement at the end of construction

Geogrid layer	Maximum tensile force (kN/m)			Horizontal Geogrid displacement at stage 6 (mm)		
	Measured (Abu-Hejleh et al. 2002)	Simulated (Zheng et al. 2016)	Current study (FEM)	Measured (Abu-Hejleh et al. 2002)	Simulated (Fakharian et al. 2007)	Current study (FEM)
6	7.7	5.7	5.13	17.01	18.37	21.18
10	8.2	4.1	4.37	19.55	17.20	23.51

5.4.4 Facing displacements and failure analysis

The maximum horizontal displacement of the facing due to the placement of bridge super structure (Stage 2 to Stage 6) is at an elevation of 4 m from the bottom and it is observed to be 13 mm from the current study. The measured horizontal displacement of the facing for the Founders Bridge due to the placement of super structure is at an elevation of 3.8 m and it is observed to be 10 mm. The outward displacements of the facing due to the placement of bridge super structure (Stage 6) alone are shown in Figure 5.6. The Total displacements after the application superstructure load is shown in Figure 5.7.

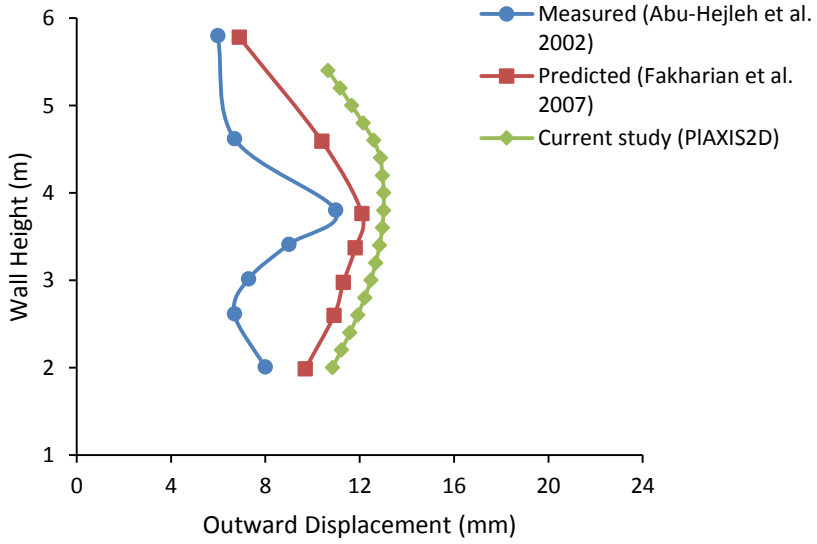

Figure.5.6: Outward displacements of the facing

The failure analysis is carried on the bridge abutment using PLAXIS 2D and LimitState:GEO. The FOS's obtained from FEM and LA methods are 2.08 and 2.451 respectively. Figure 5.7 and figure 5.8 shows the failure pattern from FEM and LA methods.

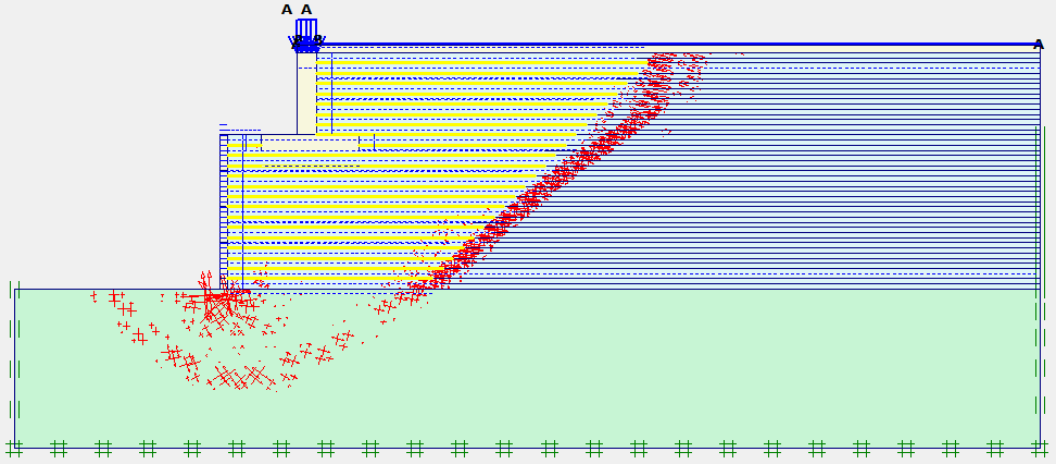

Figure.5.7: Incremental strains after safety analysis in PLAXIS 2D

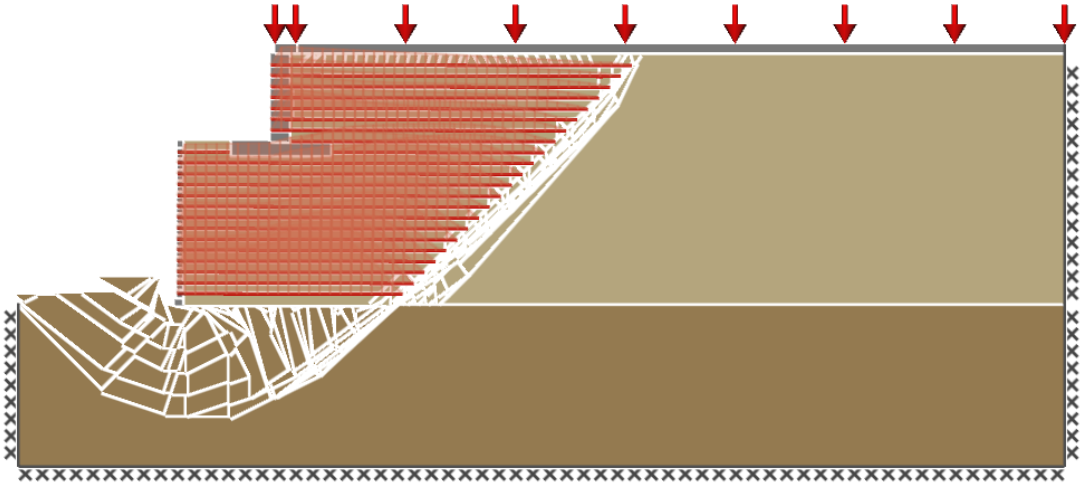

Figure.5.8: Failure surface obtained by LimitState:GEO

Chapter 6

Stability Analysis of Bridge Abutment with Surcharge

A reinforced soil wall is assumed which is of 6m in height with backfill soil resting on the unyielding foundation. An inextensible Geogrid is used as a reinforcement and the backfill is of cohesionless soil. In PLAXIS 2D while modelling the horizontal extent of the wall is assumed to 20m to reduce the boundary effect, the foundation depth is considered to be 5m and at the front of the facing the foundation is extended to a length of 5m. The bottom portion of the wall is fixed in both vertical and horizontal directions, the right side and left side boundary in fixed in horizontal direction throughout. The properties of the backfill are same as that of used for the parametric study. A footing of width 2m and height 0.3m is placed on the wall with a nominal surcharge load of 10kN/m^2 over the length of the footing. This load can be analogous to the load coming from the bridge superstructure over the footing to the abutment. The geometry of the RSW with the surcharge is shown in figure 6.1.

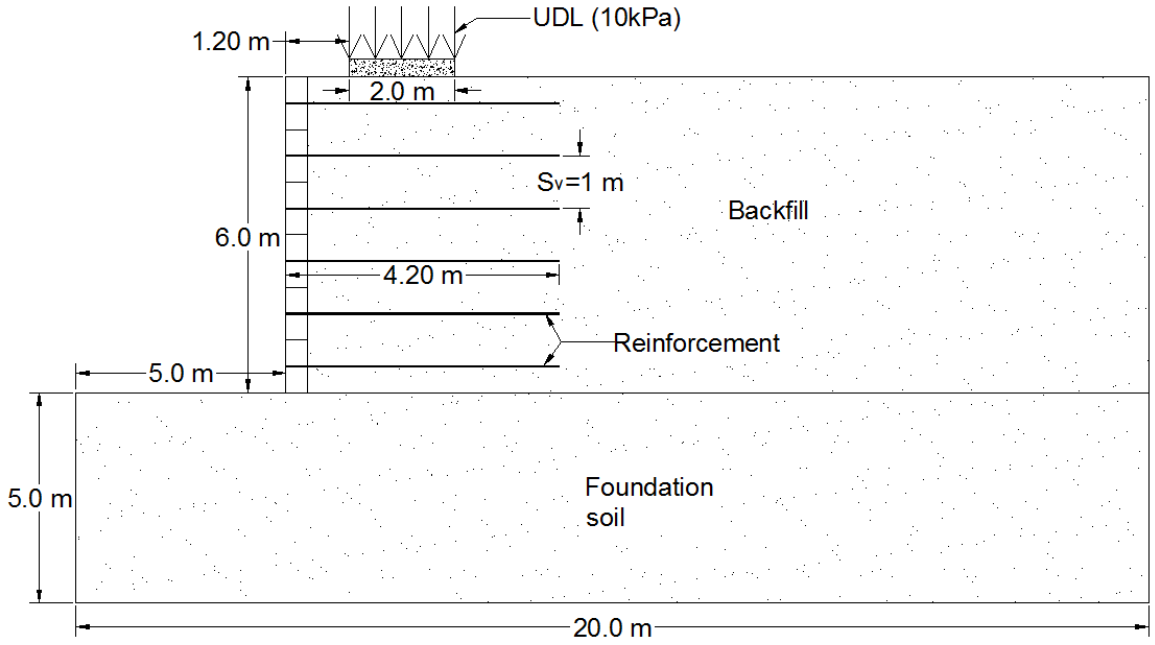

Figure.6.1: Geometry of the RSW with surcharge

The surcharge load is considered to be acting at a setback distance (D) from the facing in terms of the height of the wall (D/H=0.15, 0.2, 0.4, 0.6, 0.8). For these setback distances the deformation analysis is carried out using FEM and the safety analysis is carried out using FEM and LA. The range of the parameters is shown in Table 1. The modelled RSW in PLAXIS 2D is shown in figure 6.2.

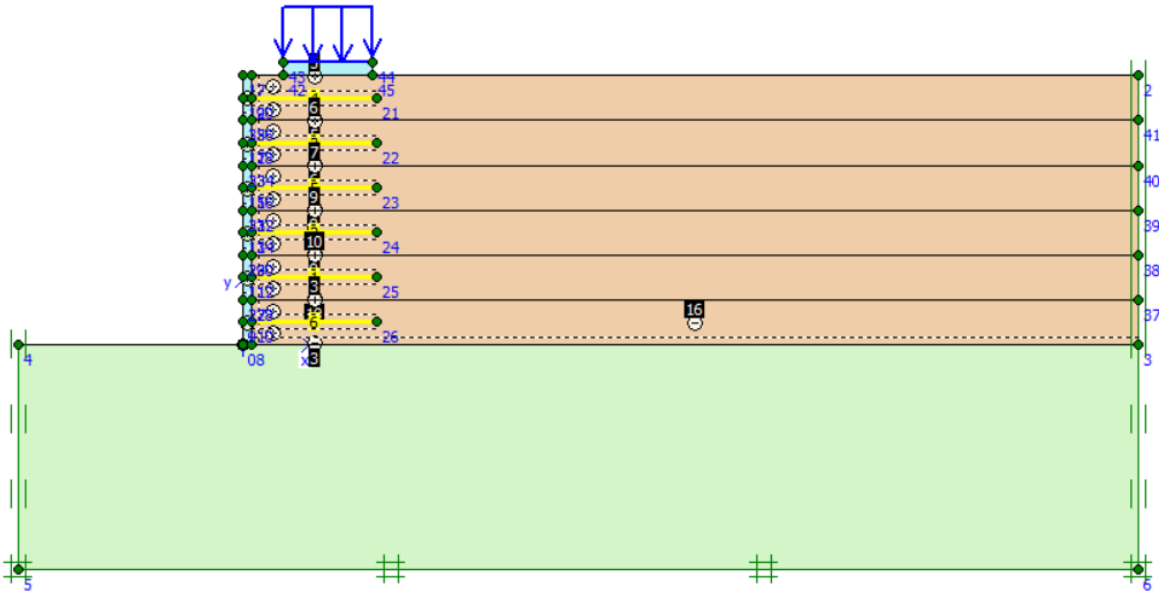

Figure.6.2: Geometry of the wall with surcharge modelled in PLAXI2D

6.1 Safety analysis

From the safety analysis the FOS values are obtained from FEM and LA. Table 6.1 shows the FOS values from PLAXIS 2D and table 6.2 shows the FOS values obtained from LimitState:GEO for different set back distances and different properties of the backfill soil. It is observed that the FOS values obtained from FEM are less when compared to the LA, this is because the LA is based on the upper bound theorem.

Table.6.1: FOS values from PLAXIS 2D

Gamma, γ (kN/m^3)	FOS				
	D/H=0.15	D/H=0.2	D/H=0.4	D/H=0.6	D/H=0.8
16	1.247	1.213	1.108	1.083	1.131
18	1.233	1.209	1.110	1.088	1.132
20	1.222	1.198	1.110	1.090	1.131
22	1.213	1.190	1.114	1.092	1.131

Phi, φ (degrees)	FOS				
	D/H=0.15	D/H=0.2	D/H=0.4	D/H=0.6	D/H=0.8
30	1.233	1.209	1.110	1.088	1.132
35	1.473	1.443	1.322	1.297	1.347
45	2.034	1.995	1.824	1.789	1.853
55	2.765	2.71	2.505	2.447	2.541

L/H	FOS				
	D/H=0.15	D/H=0.2	D/H=0.4	D/H=0.6	D/H=0.8
0.5	1.233	1.209	1.110	1.088	1.132
0.6	1.427	1.426	1.336	1.236	1.263
0.7	1.535	1.542	1.492	1.371	1.346
0.8	1.656	1.652	1.651	1.53	1.452
0.9	1.749	1.756	1.758	1.696	1.56

No of reinforcement (n)	FOS				
	D/H=0.15	D/H=0.2	D/H=0.4	D/H=0.6	D/H=0.8
4	1.113	1.09	1.011	1.024	1.054
6	1.233	1.209	1.110	1.088	1.132
8	1.276	1.250	1.157	1.114	1.150
10	1.335	1.316	1.210	1.143	1.177

R_{inter}	FOS				
	D/H=0.15	D/H=0.2	D/H=0.4	D/H=0.6	D/H=0.8
0.67	1.233	1.209	1.110	1.088	1.132
0.8	1.291	1.261	1.161	1.137	1.18
0.9	1.316	1.283	1.185	1.161	1.197
1	1.322	1.294	1.189	1.169	1.203

Table.6.2: FOS values from LimitState:GEO

Gamma, γ (kN/m^3)	FOS				
	D/H=0.15	D/H=0.2	D/H=0.4	D/H=0.6	D/H=0.8
16	1.302	1.286	1.156	1.143	1.174
18	1.290	1.276	1.157	1.146	1.174
20	1.279	1.267	1.159	1.149	1.173
22	1.271	1.259	1.160	1.150	1.173

Phi, φ (degrees)	FOS				
	D/H=0.15	D/H=0.2	D/H=0.4	D/H=0.6	D/H=0.8
25	1.053	1.041	0.945	0.936	0.958
30	1.290	1.276	1.157	1.146	1.174
35	1.551	1.535	1.392	1.378	1.412
45	2.168	2.147	1.959	1.940	1.980

L/H	FOS				
	D/H=0.15	D/H=0.2	D/H=0.4	D/H=0.6	D/H=0.8
0.4	1.106	1.078	1.004	1.028	1.067
0.5	1.290	1.276	1.157	1.146	1.174
0.6	1.438	1.436	1.343	1.262	1.282
0.7	1.563	1.565	1.524	1.399	1.385
0.8	1.684	1.684	1.668	1.569	1.483

No of reinforcement (n)	FOS				
	D/H=0.15	D/H=0.2	D/H=0.4	D/H=0.6	D/H=0.8
4	1.173	1.160	1.075	1.079	1.117
6	1.290	1.276	1.157	1.146	1.174
8	1.372	1.358	1.230	1.203	1.221
10	1.423	1.395	1.270	1.225	1.239

R_{inter}	FOS				
	D/H=0.15	D/H=0.2	D/H=0.4	D/H=0.6	D/H=0.8
0.67	1.290	1.276	1.157	1.146	1.174
0.8	1.360	1.346	1.224	1.210	1.236
0.9	1.403	1.390	1.267	1.251	1.273
1	1.436	1.424	1.305	1.285	1.303

6.1.1 Effect of unit weight and interface coefficient (R_{inter})

From the analysis it is observed that the wall is failing by overturning. In analytical study the unit weight doesn't affect the FOS for overturning failure, but from the present study it is observed that with the increase in unit weight the FOS reduces for a setback distance of D/H=0.15 and D/H=0.2 and it increases with unit weight for D/H=0.4 and D/H=0.6 and almost remains constant at D/H=0.8. Figure 6.3 shows the variation of FOS with unit weight for setback distances of D/H=0.15, D/H=0.4 and D/H=0.8 respectively.

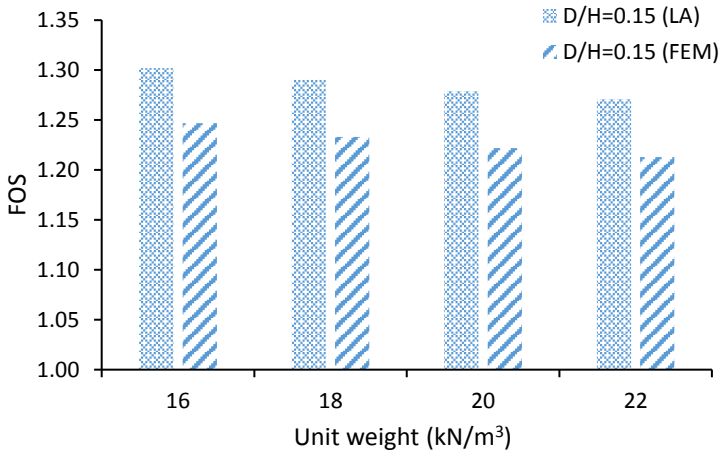

(a)

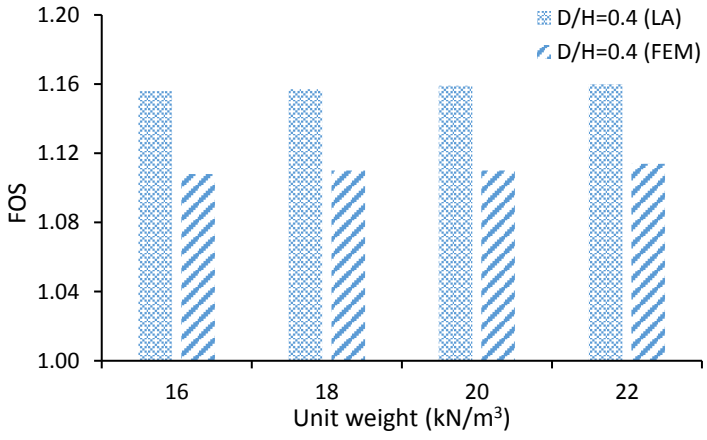

(b)

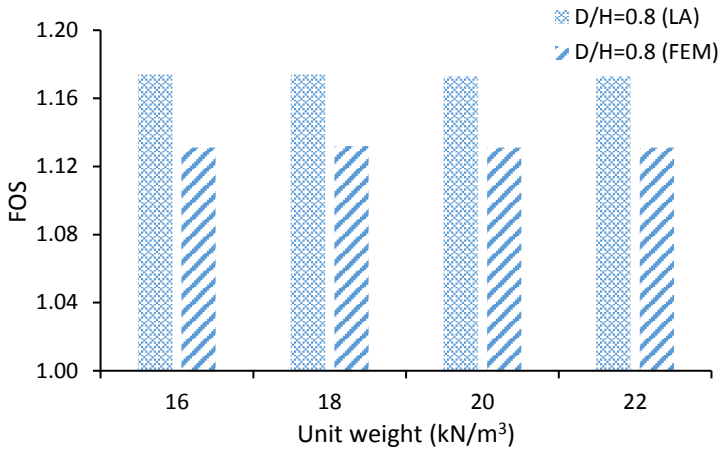

(c)

Figure.6.3: Variation of FOS with unit weight (a) D/H=0.15 (b) D/H=0.4 and (c) D/H=0.8

Figure 6.4 shows the variation of FOS with an increase in setback distance for a backfill unit weight of 18kN/m^3, φ=30^0, L/H=0.5 and for 6 number of reinforcement. It is found that the FOS decreases with increase in setback distance until D/H=0.6. For the value of D/H=0.8 the FOS is increased. The same trend is observed even for the higher unit weight of backfill soil.

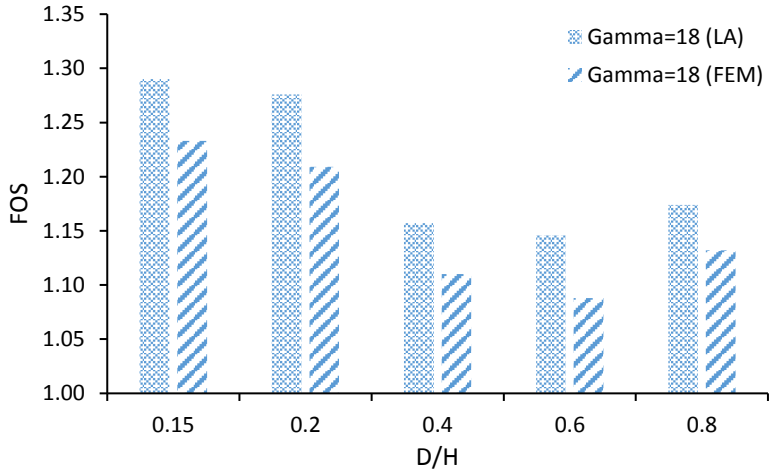

Figure.6.4: Variation of FOS with setback distance for unit weight 18kN/m^3

The increase in the interface coefficient between the backfill and reinforcement increases the FOS for a specific setback distance being all other parameters remains constant. The variation of FOS with interface for D/H=0.15 by FEM and LA are shown in figure 6.5.

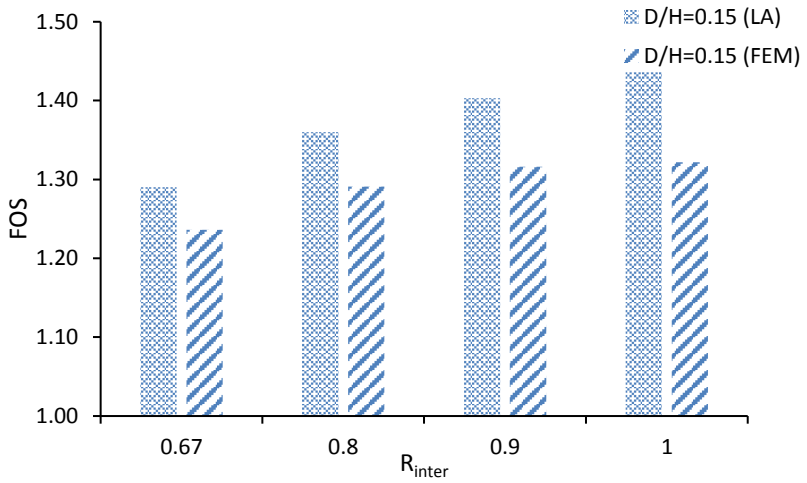

Figure.6.5: Variation of FOS with interface coefficient for D/H=0.15

6.1.2 Effect of friction angle

As the friction angle increase there will be more interlocking between the soil particles which results in an increase in FOS. Figure 6.6 shows the variation of FOS with the friction angle of backfill for D/H=0.15 from LA and FEM. From the figure it can be seen that with the increase in backfill friction angle the FOS increases. The same trend is observed for the rest of setback distances.

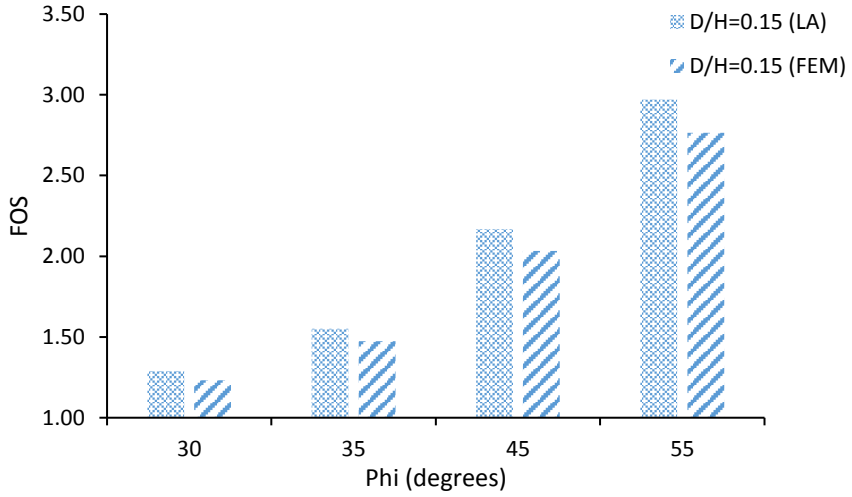

Figure.6.6: Variation of FOS with friction angle of backfill

6.1.3 Effect of number of reinforcement

As the number of reinforcement increases it is obvious that the resistance against failure will increase which in turn increases the FOS. Compared to the other parameters like friction angle and length of reinforcement the increase in the number of reinforcement has less effect on the increase of FOS. The variation of FOS with the number of reinforcement is shown in figure 6.7.

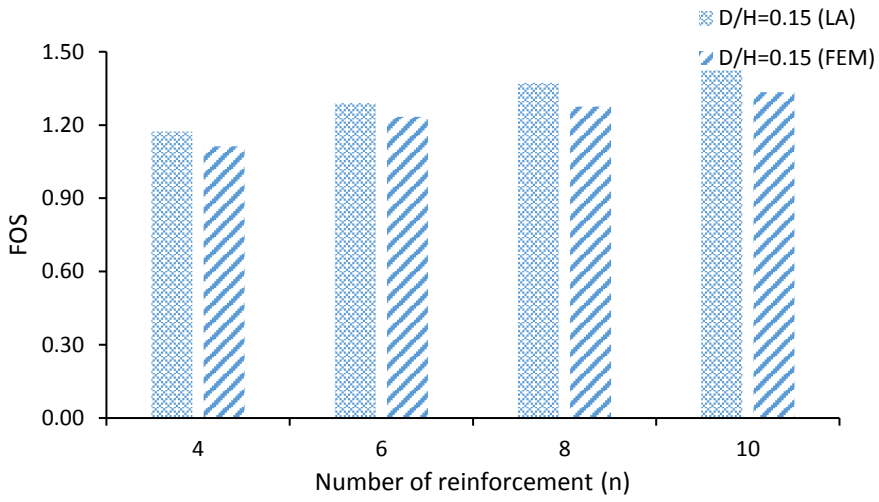

Figure.6.7: Variation of FOS with number of reinforcement

The increase in the number of reinforcement is effective when the setback distance is less i.e when the footing is near facing of the wall (Figure 6.8). As the setback distance increases the variation in the FOS reduces with the increase in the number of reinforcement.

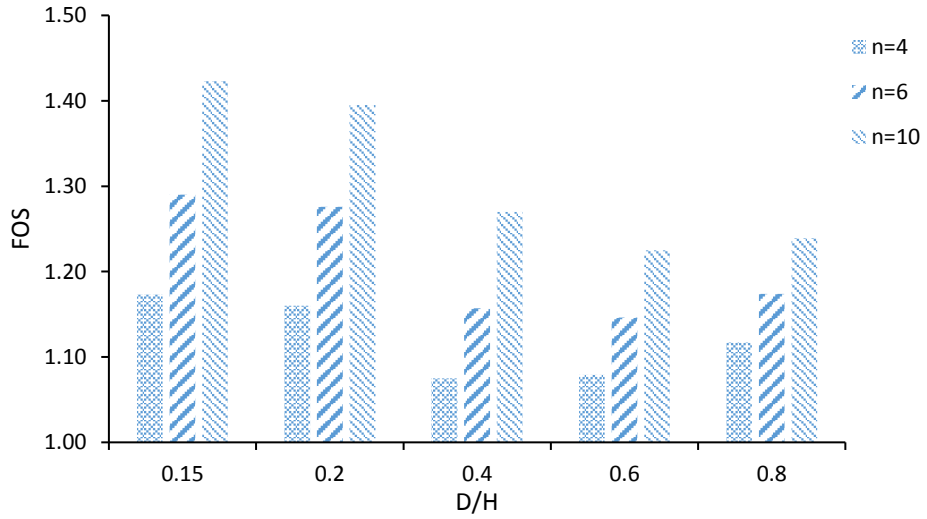

Figure.6.8: Variation of FOS with setback distance and number of reinforcement

6.1.4 Effect of length of reinforcement

The increase in the length of reinforcement increases the pull out resistance of the reinforcement and thus increases FOS. The variation of FOS with the length of reinforcement is shown in figure 6.9.

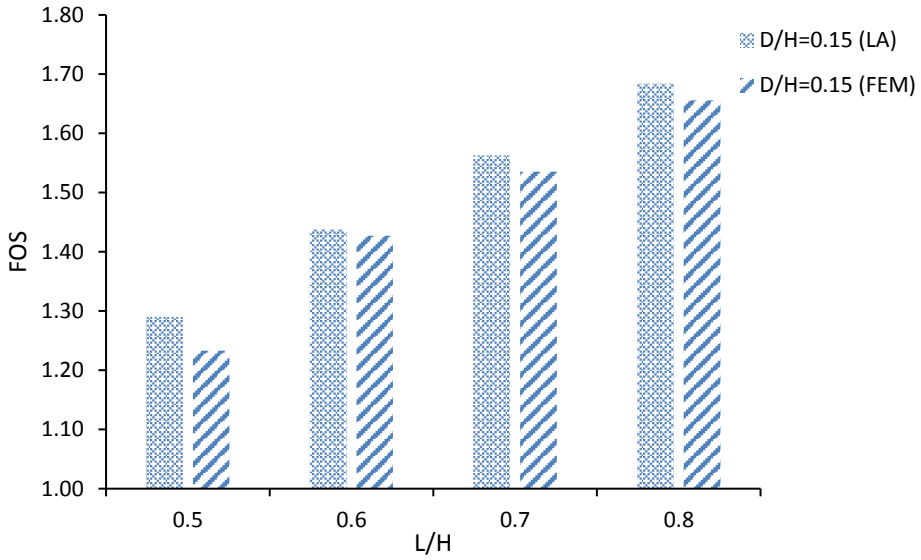

Figure.6.9: Variation of FOS with length of reinforcement

When the reinforcement length is higher there is a constant decrease in the FOS with the increase in setback distance. When the length is greater the load coming onto soil is mostly taken by the reinforced soil zone. For higher setback distance on the application of surcharge the reinforced zone as a whole tries to move away from the unreinforced zone, which induces more stress on facing wall and thus reduces the FOS. For lesser reinforcement length on increasing the setback distance, most of the load is taken by the unreinforced soil zone which induces less stress on the facing wall. This effect is observed at a distance of D/H=0.8. For the lesser reinforcement length the FOS reduces up to a setback distance of D/H=0.6. Figure 6.10 shows the variation of FOS with setback distance and length of reinforcement.

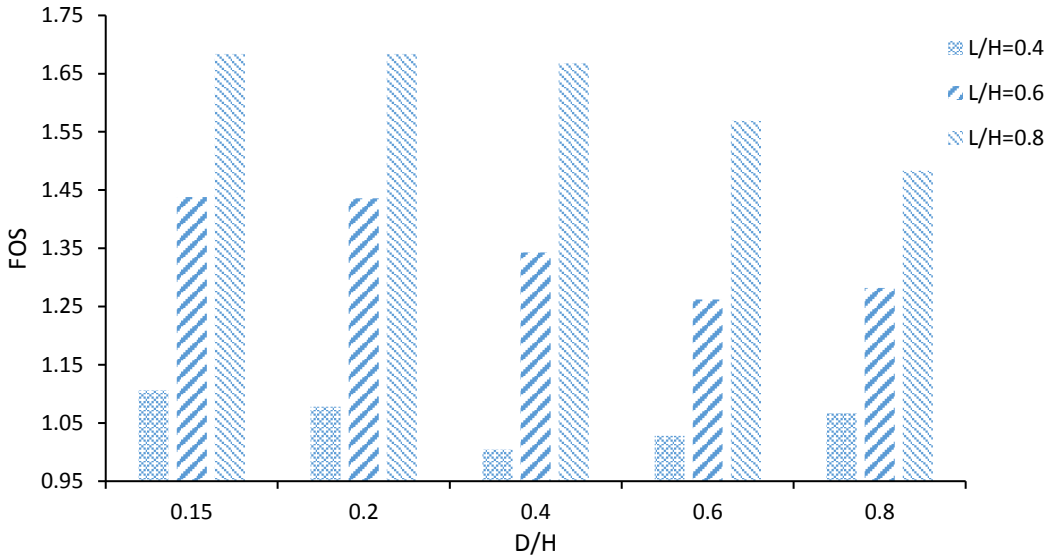

Figure.6.10: Variation of FOS with setback distance and length of reinforcement

6.1.5 Analysis of failure surfaces

The failure analysis has been done and the failure surfaces are obtained from the PLAXIS 2D and LimitState:GEO. For the case of 6 number of reinforcement, unit weight of 18kN/m^3, and friction angle of 30^0, the variation of slip lines upon varying the setback distances are shown in figure 6.10.

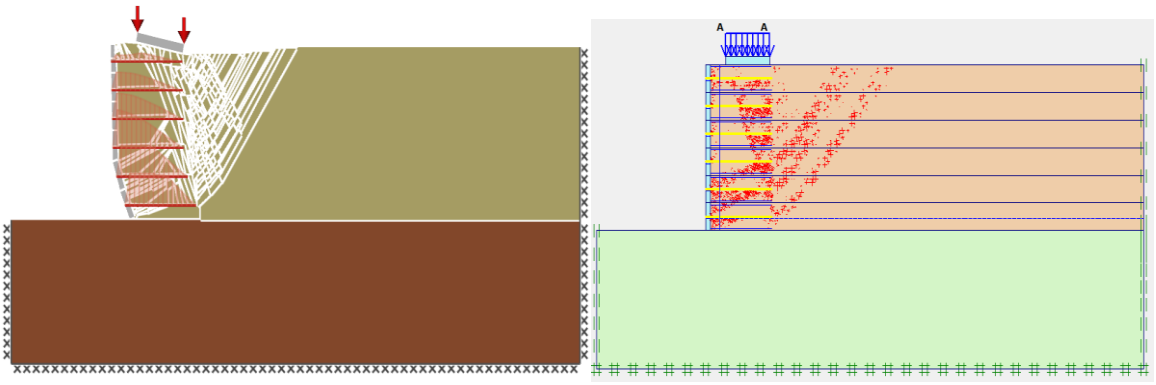

(a)

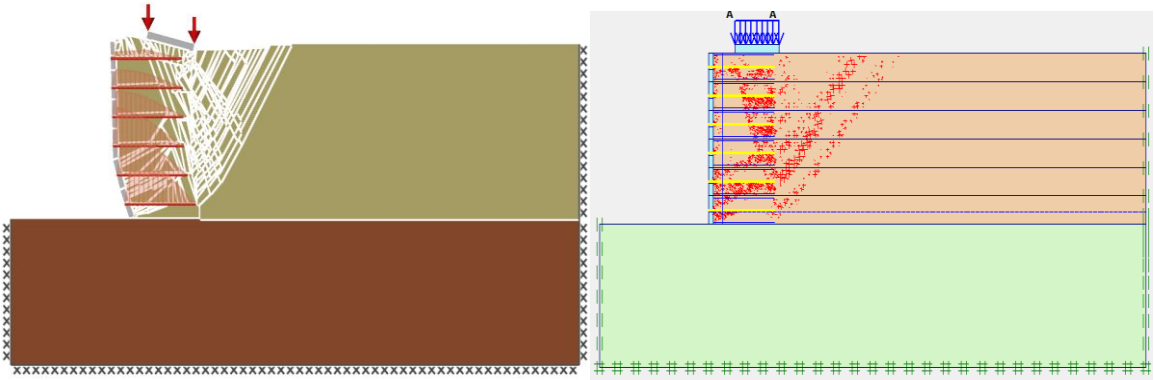

(b)

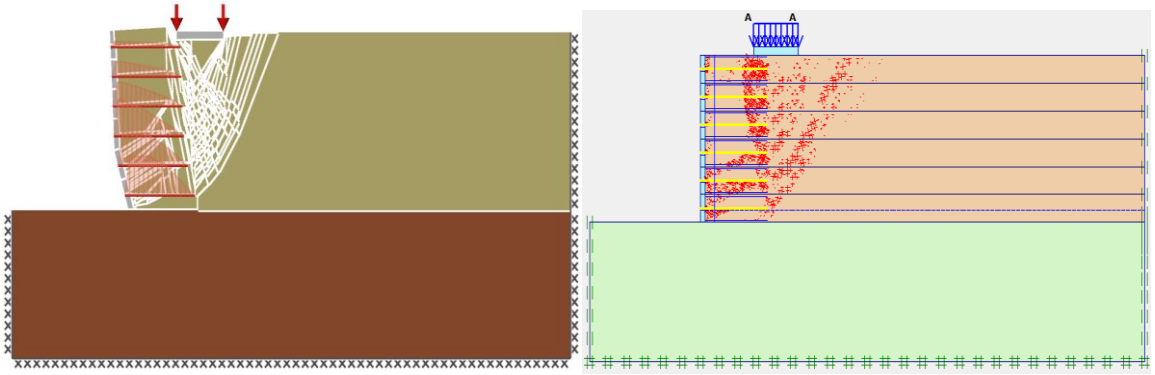

(c)

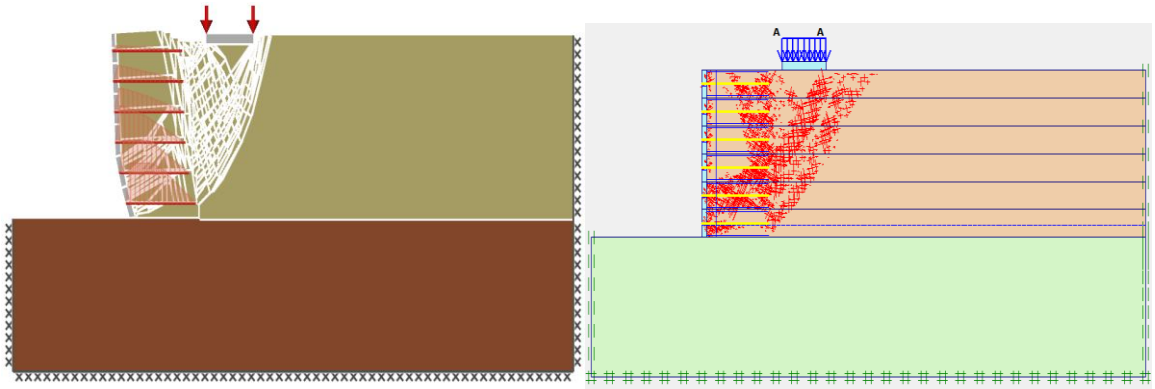

(d)

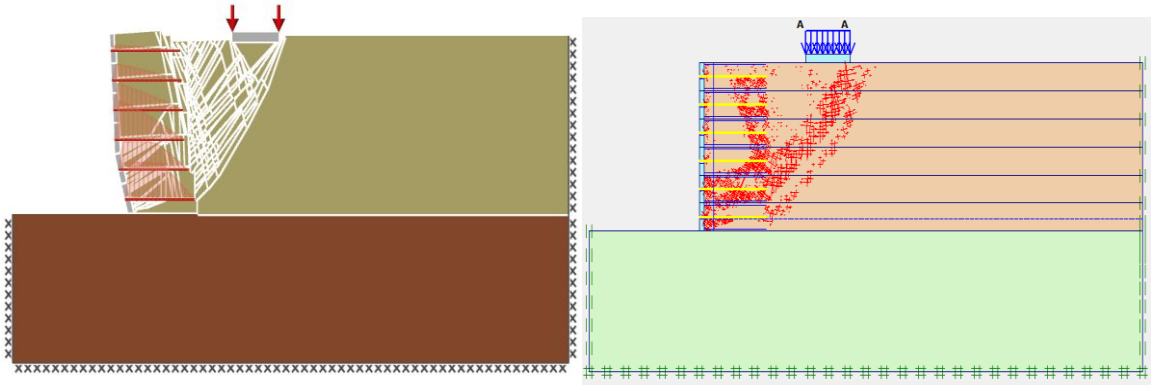

(e)

Figure.6.11: Variation of slip lines with the setback distance (a) D/H=0.15 (b) D/H=0.2 (c) D/H=0.4 (d) D/H=0.6 (e) D/H=0.8

From this study it is observed that with the increase in the setback distance, the FOS is decreased up to a value of D/H=0.6 after that for D/H=0.8 its value is increased. This is because, when the setback distance is increased the load has the tendency to move the wall facing away from the backfill because of the applied surcharge on the footing which causes the reduction in FOS of the wall. If the distance is increased further the effect of the load on the wall facing is reduced which increases the FOS. Furthermore when the setback distance is less the failure surface starts at a point away from the right edge of the footing. The failure surface starts from the edge of the footing with the increase in the setback distance and passes through the bottom most reinforcement.

6.2 Deformation analysis

The deformation analysis is carried out using PLAXIS 2D and the displacements in the reinforcement at different heights are obtained.

6.2.1 Effect of unit weight and interface coefficient (R_{inter})

The displacements in the reinforcement are observed to be increasing from the top and are maximum in the grid with an elevation of 3.5m and again reduces to a minimum at the bottom most reinforcement. The variation in reinforcement displacement with the unit weight for a setback distance of D/H=0.15 is shown in figure 6.12. It is observed that the increase in the unit weight increases the displacement in the reinforcement. The increase in the interface between reinforcement and backfill reduces the displacement in the

reinforcement (Figure 6.13). The increase in interface value increases the frictional resistance between backfill and reinforcement, this reduces the displacement in the reinforcement. The range of decrease in the displacement value is much lesser with the increase in interface compared to that of unit weight.

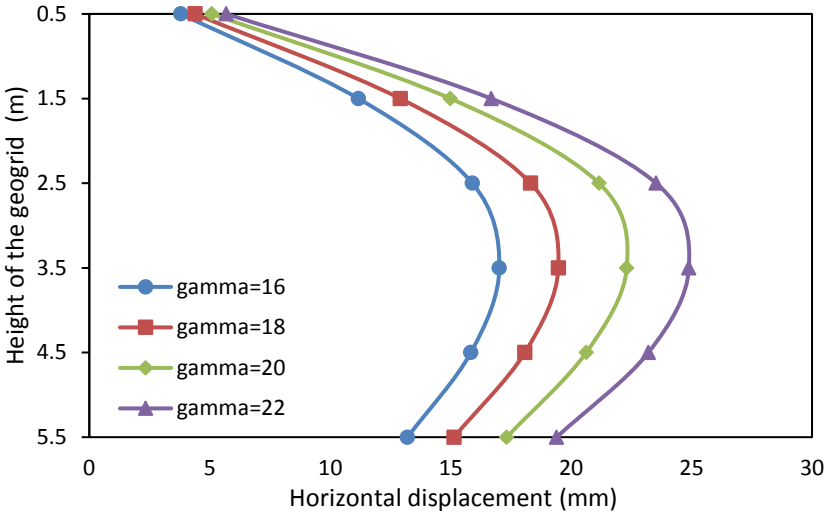

Figure.6.12: Variation of reinforcement displacement with unit weight for D/H=0.15

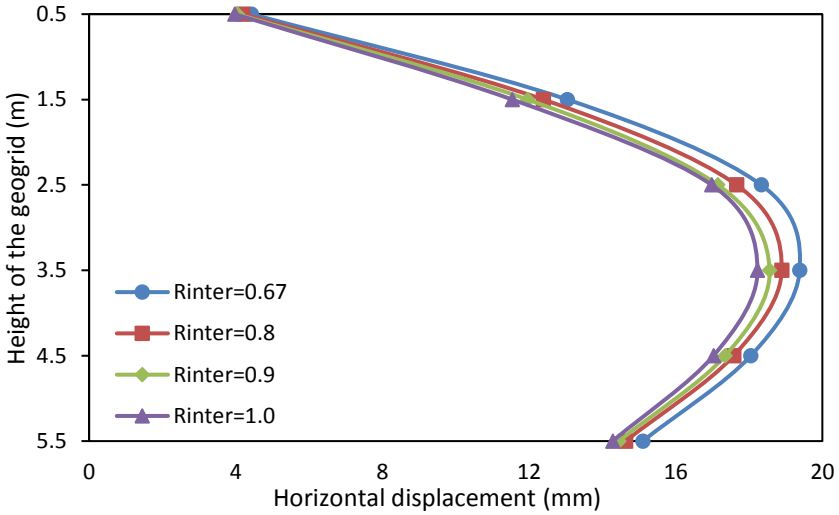

Figure.6.13: Variation of reinforcement displacement with interface (R_{inter}) for D/H=0.15

6.2.2 Effect of friction angle

The friction angle of the backfill has a considerable effect in reducing the displacement of geogrids (Figure 6.14). Compared to the all the other parameters friction angle has the maximum contribution in reducing the displacements in geogrids. The maximum

displacement is observed to be in the grid with an elevation of 3.5m from the bottom of the wall. The increase in friction angle increase the interlocking between soil particles and it reduces the pressure acting on the facing of the wall. This leads to a reduction of displacements in geogrids.

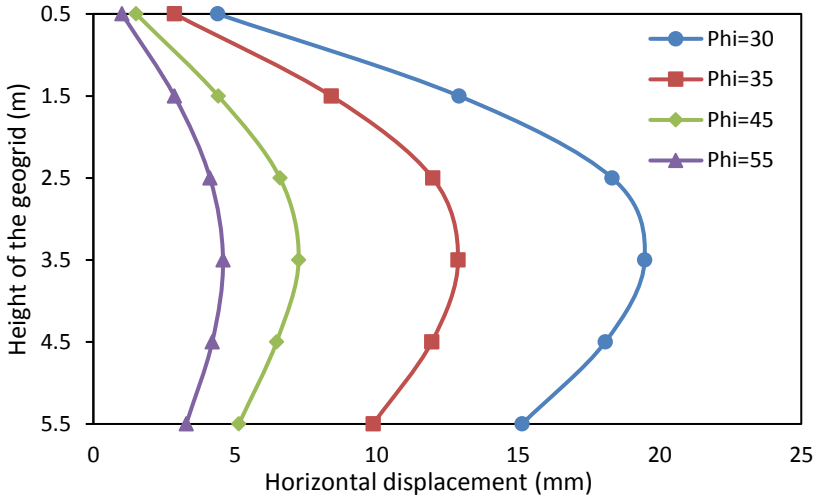

Figure.6.14: Variation of reinforcement displacement with friction angle (φ) for D/H=0.15

Figure 6.15 shows the variation in reinforcement displacement with an increase in the setback distance for $\varphi=30^0$, $\varphi=35^0$, $\varphi=45^0$, and for $\varphi=55^0$. It is observed that for $\varphi=30^0$ the displacement in reinforcement is maximum at D/H=0.6 and minimum at D/H=0.15. For $\varphi=55^0$ the displacement is maximum at D/H=0.15 and minimum at D/H=0.8. As the friction angle is increasing the maximum displacement value are observed at lesser setback distances. This shows that the friction angle is effective in reducing the displacements when the setback distance is more.

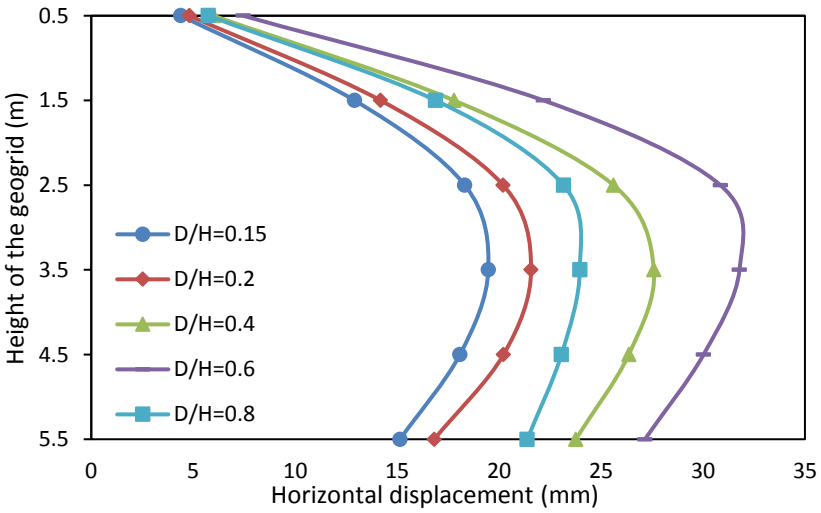

(a)

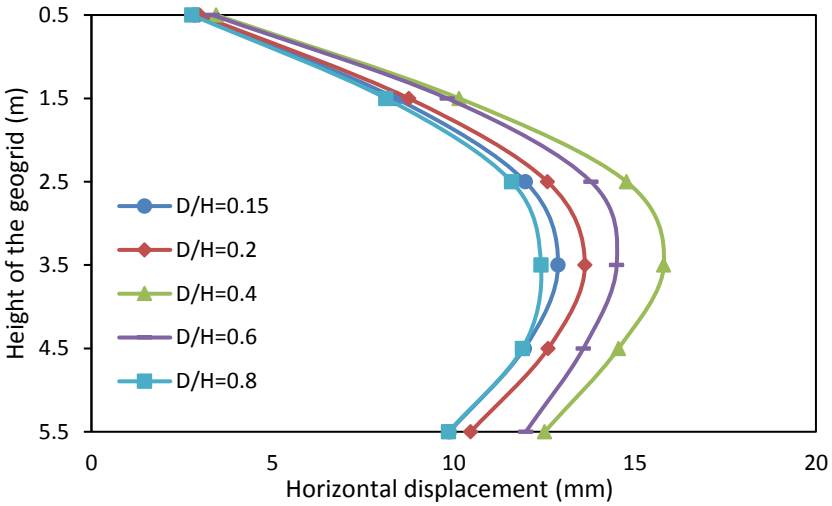

(b)

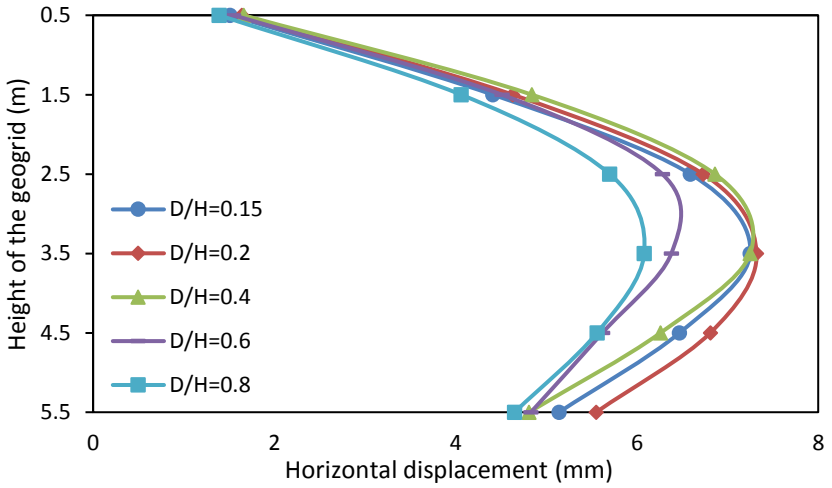

(c)

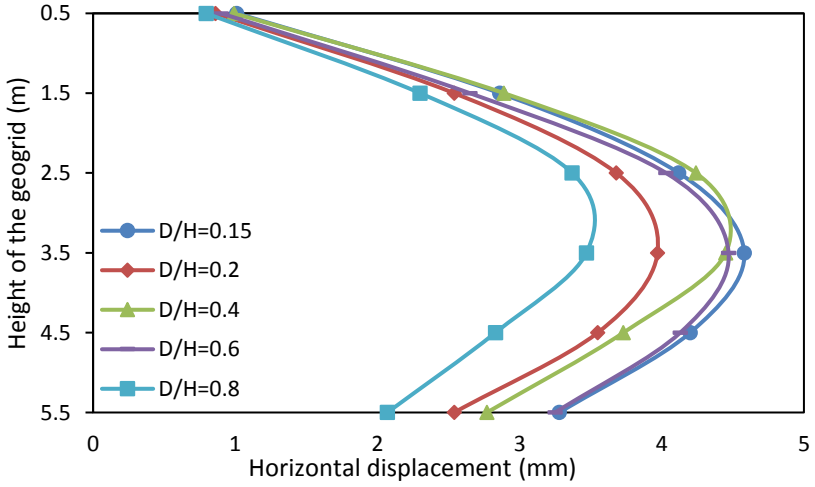

(d)

Figure.6.15: Variation of displacement in reinforcement (a) $\varphi=30^0$ (b) $\varphi=35^0$ (c) $\varphi=45^0$ (d) $\varphi=55^0$

6.2.3 Effect of number of reinforcement

With the increase in number of reinforcement the deformations in reinforcement are reduced. The deformations are almost reduced to 4 times when the number of reinforcement are increased from 4 to 10 for different setback distances (Figure 6.16). In the case of 4 number of reinforcement the maximum displacement is observed at D/H=0.4 and for a higher number of reinforcement maximum displacement is observed at D/H=0.6.

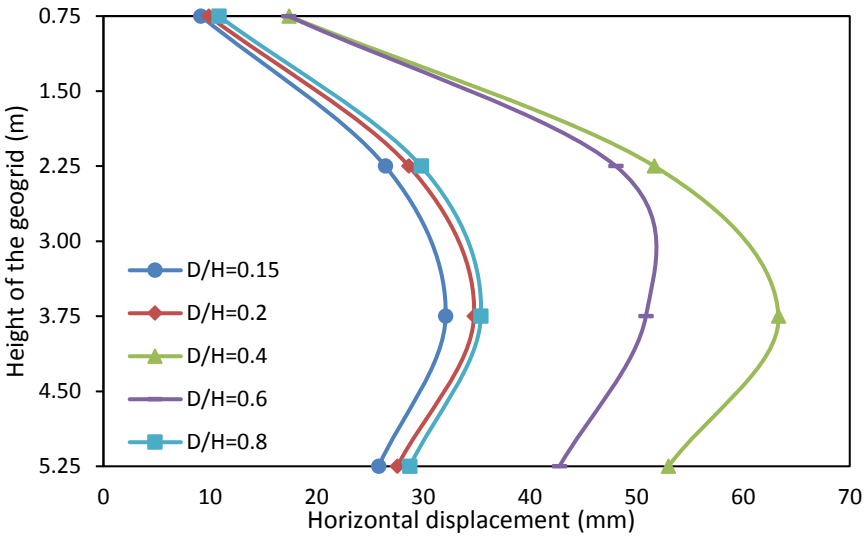

(a)

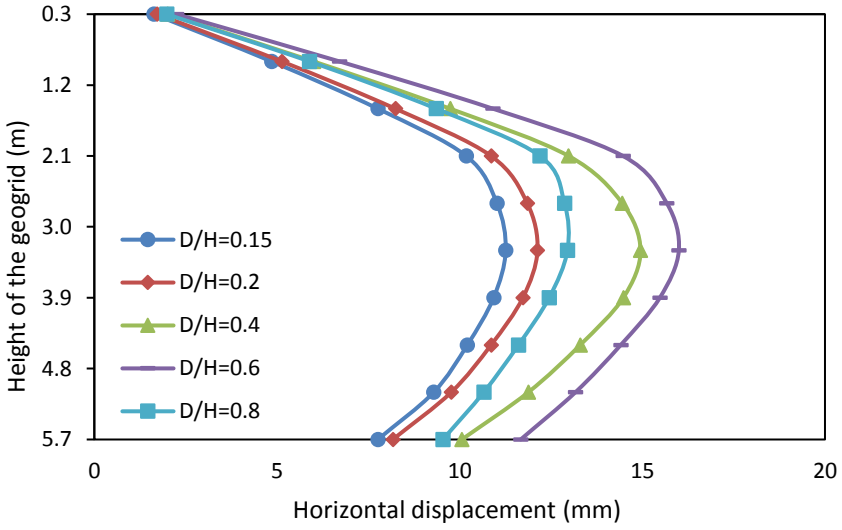

(b)

Figure.6.16: Variation of displacement in reinforcement (a) n=4 (b) n=10

6.2.4 Effect of length of reinforcement

With the increase in the length of reinforcement the resistance against pullout increases which reduces the stress on the wall, this causes the reduction of the displacement in the geogrid. The length of reinforcement has a significant effect on reducing the displacement with increase in setback distance. As the reinforcement length is higher the decrease in displacement of the grid with setback distance is found to be reduced (Figure 6.17).

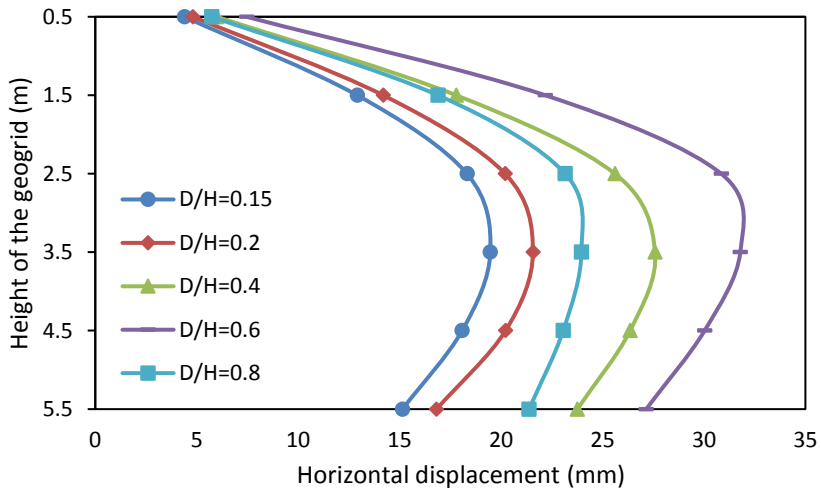

(a)

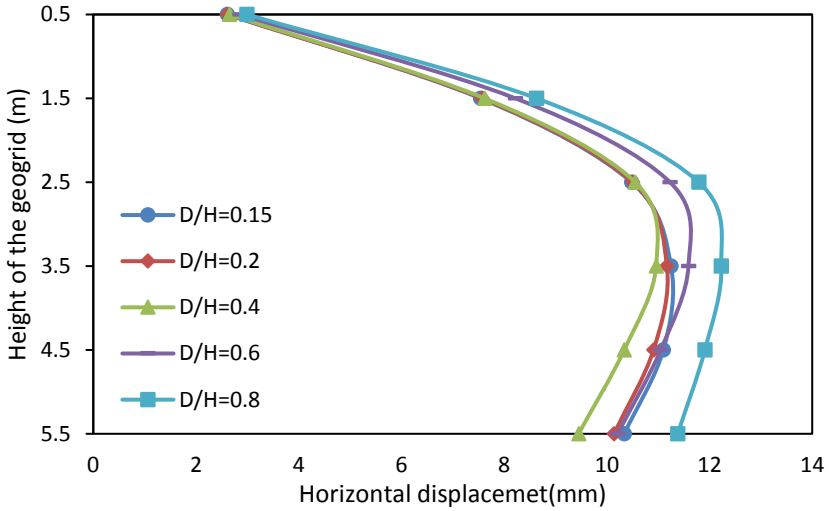

(b)

Figure.6.17: Variation of displacement in reinforcement (a) L/H=0.5 (b) L/H=0.8

Chapter 7

Conclusion and Future Scope

7.3 Conclusions

Based on the present the following conclusions are drawn:

1. From the parametric study of reinforced soil wall, it is observed that the effect of friction angle on the increase in FOS is more compared to the other parameters.
2. The FOS's obtained from the LimitState:GEO analysis is higher than those obtained from PLAXIS 2D. This is because LimitState:GEO works based on the principle of limit analysis which gives higher values compared to FEM analysis.
3. The obtained values from FEM analysis are in good agreement with the measured values of case studies. The facing wall displacement and grid loads in the case of bridge abutment are almost equivalent with the measured values. This gives a confidence that the numerical analysis can be effectively used for these type of studies.
4. From the study of reinforced soil wall as bridge abutment the following conclusions are drawn for safety and deformation analysis.
   - **4.1** For lesser set back distance (D/H=0.15 and D/H=0.2) with an increase in weight the FOS is reduced and attains a constant value when the setback distance is more (D/H=0.8) irrespective of unit weight variation. The displacement in the reinforcement is increasing with increase in the unit weight for a particular setback distance.
   - **4.2** With the increase in the backfill friction angle the FOS is increasing and there is a reduction in the displacement of geogrid. When the setback distance is more the increase in friction angle is effective in reducing the displacements
   - **4.3** The increase in number of reinforcement has less effect in increasing the FOS compared to other parameters (backfill friction angle and length of reinforcement). This is effective for lesser setback distance, as the setback distance is higher the increase in FOS reduces with increase in number of reinforcement. The maximum deformations in the reinforcement are almost

reduced to 4 times when the number of reinforcement are increased from 4 to 10.

4.4 For the higher reinforcement length (L/H=0.8) the FOS is reducing continuously on increasing the setback distance. The setback distance has a significant effect on reducing the displacements in the grid for lesser reinforcement length.

4.5 The FOS of the wall is increasing with the increase in the interface coefficient between backfill and reinforcement and the displacement of the geogrid is reduced for a particular setback distance.

7.4 Scope for further study

The scope for the application of GRS walls in the bridge abutment is considerably significant in the present scenario. The present study is mainly concentrated on the effect of different parameters of the backfill on RSW. The following aspects should be considered for the future study.

1. The study of the wall by considering cohesive backfill soil.
2. Differential settlements between the abutment and the approaching roadway can be studied.
3. The present study doesn't consider the effect of the ground water table, so the effect of ground water table on the behaviour of abutment can be studied.

Bibliography

1. AASHTO (2002). *Standard specifications for highway bridges*, 17th edn, American Association of State Highway and Transportation Officials (AASHTO), Washington, DC.

2. Abu-Hejleh, N., Zornberg, J.G., Wang, T., & Watcharamonthein, J. (2002). Monitored displacements of unique geosynthetic-reinforced soil bridge abutments, *Geosynthetics International, 9(1),* 71-95.

3. Bathurst, R. J., Nernheim, A., Walters, D. L., Allen, T. M., Burgess, P., & Saunders, D. D. (2009). Influence of reinforcement stiffness and compaction on the performance of four geosynthetic-reinforced soil walls. *Geosynthetics International*, *16*(1), 43-59.

4. Bhandari, A., & Han, J. (2010). Investigation of geotextile–soil interaction under a cyclic vertical load using the discrete element method. *Geotextiles and geomembranes*, *28*(1), 33-43.

5. Bilgin, Ö. (2009). Failure mechanisms governing reinforcement length of geogrid reinforced soil retaining walls. *Engineering Structures*, *31*(9), 1967-1975.

6. Ehrlich, M., Mirmoradi, S. H., & Saramago, R. P. (2012). Evaluation of the effect of compaction on the behavior of geosynthetic-reinforced soil walls. *Geotextiles and Geomembranes*, *34*, 108-115.

7. Fahel, A. R., Palmeira, E. M., & Ortigao, J. A. R. (2000). Behaviour of geogrid reinforced abutments on soft soil in the BR 101-SC highway, Brazil. In *Advances in Transportation and Geoenvironmental Systems Using Geosynthetics* (pp. 257-270).

8. Fakharian, K., & Attar, I. H. (2007). Static and seismic numerical modeling of geosynthetic-reinforced soil segmental bridge abutments. *Geosynthetics International*, *14*(4), 228-243.

9. Grien, M. J., Truong, K., & Tavakolian, M. R. (2010). Study of Mechanically Stabilized Earth Structure Supporting Integral Bridge Abutment. In *Earth Retention Conference 3* (pp. 772-779).

10. Guler, E., Cicek, E., Demirkan, M. M., & Hamderi, M. (2012). Numerical analysis of reinforced soil walls with granular and cohesive backfills under cyclic loads. *Bulletin of Earthquake Engineering*, *10*(3), 793-811.

11. Guler, E., Hamderi, M., & Demirkan, M. M. (2007). Numerical analysis of reinforced soil-retaining wall structures with cohesive and granular backfills. *Geosynthetics International*, *14*(6), 330-345.

12. Hatami, K., Bathurst, R. J., & Pietro, P. D. (2001). Static response of reinforced soil retaining walls with nonuniform reinforcement. *International Journal of Geomechanics*, *1*(4), 477-506.

13. Helwany, S. M., Wu, J. T., & Froessl, B. (2003). GRS bridge abutments—an effective means to alleviate bridge approach settlement. *Geotextiles and Geomembranes*, *21*(3), 177-196.

14. Kumar, P. V. S. N. P., & Madhav, M. R. (2009). Analysis of reinforced soil wall considering oblique pull: bilinear failure mechanism—Linear subgrade response. *Lowland Technology International*, *11*(1), 1-11.

15. Lackner, C., Bergado, D. T., & Semprich, S. (2013). Prestressed reinforced soil by geosynthetics–Concept and experimental investigations. *Geotextiles and Geomembranes*, *37*, 109-123.

16. LimitState:GEO–version 3.4.a (2016). *LimitState:GEO Manual*, LimitState Ltd, Sheffield, United Kingdom.

17. Lovisa, J., Shukla, S. K., & Sivakugan, N. (2010). Behaviour of prestressed geotextile-reinforced sand bed supporting a loaded circular footing. *Geotextiles and Geomembranes*, *28*(1), 23-32.

18. Mirmoradi, S. H., & Ehrlich, M. (2014). Numerical evaluation of the behavior of GRS walls with segmental block facing under working stress conditions. *Journal of Geotechnical and Geoenvironmental Engineering*, *141*(3), 04014109.

19. PLAXIS 2D–version 9.02 (2008). *Reference Manual*, Delft University of Technology, Delft, Netherlands.

20. Rowe, R. K., & Skinner, G. D. (2001). Numerical analysis of geosynthetic reinforced retaining wall constructed on a layered soil foundation. *Geotextiles and Geomembranes*, *19*(7), 387-412.

21. Skinner, G. D., & Rowe, R. K. (2005). Design and behaviour of a geosynthetic reinforced retaining wall and bridge abutment on a yielding foundation. *Geotextiles and Geomembranes*, *23*(3), 234-260.

22. Wu, J. T., Lee, K. Z., & Pham, T. (2006). Allowable bearing pressures of bridge sills on GRS abutments with flexible facing. *Journal of Geotechnical and Geoenvironmental Engineering*, *132*(7), 830-841.

23. Zheng, Y., & Fox, P. J. (2016). Numerical Investigation of Geosynthetic-Reinforced Soil Bridge Abutments under Static Loading. *Journal of Geotechnical and Geoenvironmental Engineering*, *142*(5), 04016004.

Dissemination

Conferences

1. Kumar, P.V.P., Patra, S. and Patel, V. (2016). “Numerical investigation of a full scale reinforced soil wall - a case study.” *5th International Conference on Forensic Geotechnical Engineering*, December 8-10, 2016, Bengaluru.
2. Patel, V., Patra, S. and Kumar, P.V.P. (2016). “Limit analysis of full scale MSE wall- a comparative study.” *Indian Geotechnical Conference*, December 15-17, 2016, Chennai.